

ADSORPTION OF Cu, Ni AND Fe ATOMS ONTO WSe₂ MONOLAYER: A DFT STUDY

Thesis submitted

In partial fulfilment of the requirements for the

Degree of

MASTER OF SCIENCE

in

Physics

by

Tripti Gupta

(2K22/MSCPHY/44)

Under the supervision of

Prof. Nitin K. Puri

(Delhi Technological University)



To the

Department of Applied Physics

DELHI TECHNOLOGICAL UNIVERSITY

(Formerly Delhi College of Engineering)

Shahbad Daultapur, Main Bawana Road, Delhi-110042, India

May,2024

**ADSORPTION OF Cu, Ni AND Fe ATOMS ONTO
WSe₂ MONOLAYER: A DFT STUDY**



DELHI TECHNOLOGICAL UNIVERSITY
(Formerly Delhi College of Engineering)
Shahbad Daultapur, Main Bawana Road, Delhi-42

ACKNOWLEDGEMENTS

I would like to express my indebtedness and deepest sense of regard to my supervisor, **Prof. Nitin K. Puri, Department of Applied Physics, Delhi Technological University** for providing his incessant expertise, inspiration, encouragement, suggestions, and this opportunity to work under his guidance. I am grateful for the constant help provided at every step of this project by all the lab members (Ph.D. scholars) of the **Nanomaterials Sensor laboratory (NSL)**, Department of Applied Physics, Delhi Technological University.

I also extend my in-depth gratitude towards our labs scholars Mr. Anurag Bhandari and Ms. Kanika, who supported me in keeping my spirits high, even when the times were very distressful. I would also like to thank our laboratory members and friends Archana Krishnan and Arun Saji, for their constant support and understanding.

I am also thankful to my family and colleagues for their invaluable support, care, and patience during this project. Lastly, I would thank Delhi Technological University for providing such a wonderful opportunity of working on this project.

Tripti Gupta

(2k22/MSCPHY/44)



DELHI TECHNOLOGICAL UNIVERSITY
(Formerly Delhi College of Engineering)
Shahbad Daulatpur, Main Bawana Road, Delhi-42

CANDIDATE'S DECLARATION

I, **Tripti Gupta (2K22/MSCPHY/44)** student of M.Sc physics, hereby certify that the work which is being presented in the thesis entitled “**Adsorption of Cu, Ni and Fe atoms onto WSe₂ monolayer: A DFT study**” in partial fulfilment of the requirement for the award of the degree of Master in Science, submitted in the Department of Applied Physics, Delhi Technological University is an authentic record of my own work carried out during the period from May 2023 to May 2024 under the supervision of Professor Nitin Kumar Puri.

The matter represented in the thesis has not been submitted by me for the award of any other degree of this or any other institute.

Tripti Gupta
(2k22/MSCPHY/44)

This is to certify that the student has incorporated all the corrections suggested by the examiner in the thesis and the statement made by the candidate is correct to the best of our knowledge.

Prof. Nitin K. Puri
(Supervisor)

Signature of External Examiner



DELHI TECHNOLOGICAL UNIVERSITY
(Formerly Delhi College of Engineering)
Shahbad Daulatpur, Main Bawana Road, Delhi-42

CERTIFICATE BY THE SUPERVISOR

Certified that **Tripti Gupta (2k22/MSCPHY/44)** has carried out the search work presented in this thesis entitled “**Adsorption of Cu, Ni and Fe atoms onto WSe₂ monolayer: A DFT study**”, for the award of **Master of Physics from Department of Applied Physics, Delhi Technological University, Delhi** under my supervision. The thesis embodies result of original work, and studies are carried out by the student herself and the content of the thesis do not form the basis for the award of any other degree to the candidate or to anybody else from this or any other university.

Prof. Nitin K. Puri
(Department of Applied Physics)
Delhi Technological University

ABSTRACT

The adsorption of 3d transition metal (TM) atoms like Cu, Ni, and Fe on the WSe₂ monolayer was investigated using first-principal calculations, specifically Density Functional Theory (DFT), which is a powerful computational approach to understand the adsorption phenomenon at the atomic level comprehensively. This study reveals that the adsorption of these TM atoms enhances the overall properties of the monolayer by affecting its geometry, adsorption energy, and electronic and magnetic properties. DFT provides insights into the changes induced by the adsorbates. Calculations were performed using the Generalized Gradient Approximation and ultrasoft pseudopotentials, evaluating three adsorption sites (H, T_W, and T_{Se}) on the monolayer. The optimal adsorption site was determined by calculating the adsorption energy for each optimized configuration. The results showed that Cu and Ni atoms prefer the T_W site, with adsorption energies of -3.05 eV and -4.72 eV, respectively, while Fe prefers the H site with an adsorption energy of -4.37 eV. These high adsorption energies indicate strong chemical adsorption, suggesting covalent bonding between the atoms and the monolayer, which significantly influences the WSe₂ monolayer's geometry and modifies its electronic and magnetic properties. A key objective was to investigate how TM atom adsorption alters the optical and electronic properties of the WSe₂ monolayer, enhancing its suitability for optoelectronic and spintronic applications. Electronic parameters such as the density of states (DOS), projected density of states (PDOS), and charge transfer were analyzed. DOS analysis revealed that the pristine WSe₂ monolayer, which has a band gap of 1.27 eV, undergoes significant band gap reduction upon TM atom adsorption. Specifically, Cu and Fe adsorption closed the band gap entirely, transforming the WSe₂ monolayer into a metallic state. In contrast, Ni adsorption reduced the band gap to 0.88 eV, indicating a transition to a narrower band gap semiconductor. This band gap modulation is crucial for tuning the electronic properties of WSe₂ for various device applications. The study also observed shifts in the Fermi energy level upon TM atom adsorption, indicating substantial changes in the monolayer's electronic structure. PDOS analysis provided more profound insights into the interactions between the TM atoms and the WSe₂ monolayer, showing significant hybridization between the 3d orbitals of the TM atoms, the 5d orbitals of W, and the 4p orbitals of Se. This strong orbital hybridization indicates robust chemical bonding, which is responsible for the variations in electronic properties. Charge density difference calculations supported these findings, showing considerable charge transfer from the TM atoms to the WSe₂ monolayer. This is a critical factor in band gap narrowing and the transition to metallic behavior. The adsorption of Cu, Ni, and

Fe on the WSe₂ monolayer enhances its electronic properties and induces magnetic properties due to the presence of unpaired d-electrons in these transition metals. This is particularly advantageous for spintronic applications, where control of spin-dependent properties is essential. The detailed understanding of the adsorption mechanism provided by this study highlights the potential of TM-doped WSe₂ monolayers as multifunctional materials engineered for specific optoelectronic and spintronic applications. The ability to modulate the band gap and introduce metallic behavior through TM atom adsorption opens new opportunities for designing devices with tailored electronic properties. Additionally, the observed changes in the Fermi level and strong covalent bonding emphasize the potential for stable and efficient material performance in practical applications. In conclusion, this study thoroughly analyses Cu, Ni, and Fe atom adsorption on the WSe₂ monolayer using DFT. The results demonstrate significant enhancements in the monolayer's electronic and magnetic properties due to strong chemical bonding and charge transfer from the adsorbates. The modulation of the band gap and the transition to metallic behavior upon TM atom adsorption suggest that TM-doped WSe₂ monolayers are promising candidates for advanced optoelectronic and spintronic devices. These insights can guide future experimental and theoretical research to optimize the properties of TMD-based materials for a wide range of technological applications.

LIST Of PUBLICATIONS

Title of Paper : ADSORPTION OF Cu, Ni AND Fe ATOMS ONTO WSe₂ MONOLAYER:
A DFT STUDY

Author Names: Tripti Gupta, Anurag Bhandari, Nitin K. Puri

Name of Conference: International Conference on Atomic, Molecular, Material, Nano and
Optical Physics 2023

Date of Conference: 20 December 2023

Status of Paper (Accepted/Published/Communicated): Communicated

Date of Communication : 5 June 2024

TABLE OF CONTENTS

Title	Page No.
Acknowledgement	iii
Candidate's Declaration	iv
Certificate by the Supervisor	v
Abstract	vi
List of Publications	viii
Table of Contents	ix
List of Tables	xi
List of Figures	xii
List of Symbols, Abbreviations and Nomenclature	xiv
1. Introduction	01
1.1 Two-Dimensional Materials	02
1.2 Transition Metal Dichalcogenides	03
1.3 WSe ₂ Monolayer	05
1.4 Doping as Strategy	06
1.5 Conclusion	06
2. Computational Methodology	08
2.1 Density Functional Theory	08
2.2 Quantum Espresso	11
2.3 Exchange-Correlational Energy	12
2.3.1 GGA	13
2.4 Convergence Tests	14
2.5 Pseudopotentials	15
2.5.1 Ultrasoft Pseudopotentials	16
2.6 Boryden-Fletcher-Goldfarb-Shanno (BFGS) Scheme	16
2.7 Computational Framework	17

2.8 Outline Of Thesis	18
3. Results and Discussion	20
3.1 Structure and Electronic properties	20
analysis of WSe ₂ Monolayer	
3.2 Adsorption of TM atoms onto	22
pristine WSe ₂ monolayer	
3.2.1 Structure and Adsorption Analysis	23
of Cu Atom onto Pristine WSe ₂ Monolayer	
3.2.2 Structure and Adsorption Analysis	24
of Ni Atom onto Pristine WSe ₂ Monolayer	
3.2.3 Structure and Adsorption Analysis of	25
Fe Atom onto Pristine WSe ₂ Monolayer	
3.2.4 Effect of Cu, Ni, and Fe Adsorption on	26
the Electronic Properties of WSe ₂ Monolayer	
3.2.5 Charge Density Difference Analysis	29
4. Conclusion and Future Scope	31
5. References	33
6. List of Publication and proof	39
7. Scopus Index	40
8. Plagiarism Report	41

List of Tables

S. No.	Table No.	Title of the Table	Page No.
1	Table 1	Adsorption sites, adsorption energy(eV), adsorption height (Å) for the optimized Cu, Ni and Fe decorated WSe ₂ monolayer respectively.	23

List of Figures

S. No.	Fig. No.	Title of the Figure	Page No.
1	1	Different types of nanomaterials on the basis of quantum confinement of electrons	2
2	2	Different types of 2D nanomaterials and their applications in various fields.	3
3	3	Four different Transition Metal dichalcogenides Monolayer(TMD ML)	4
4	4	Applications of Transition Metal dichalcogenides Monolayer(TMD ML) in various fields.	4
5	5	Top view and side view of WSe ₂ Monolayer	5
6	6	Represents (a) Substitutionally doped Monolayer and (b)Surface-Modification of Monolayer through Adsorption	6
7	7	Theme of Density Functional Theory	8
8	8	LOGO of Quantum Espresso	12
9	9	Curves representing the variation in the ground state energy with (A) K- points and (B) cut-off energy respectively.	15
10	10	(a)Top and (b) Side view of the optimized pristine WSe ₂ structure respectively. The blue and orange coloured atoms represent the W and Se atoms respectively.	20
11	11	Plotted a) DOS and b) PDOS for the pristine WSe ₂ monolayer respectively.	21
12	12	illustrates H, T _w and T _{se} adsorption sites selected for the adsorption of TM atom onto WSe ₂ monolayer respectively.	22
13	13	a),b),c) illustrates Top view and d),e),f) Side view of the optimized Cu adsorbed geometries at the T _{se} , H and T _w sites respectively. The atoms in orange, blue and red colour represents the Se, W and Cu atoms respectively.	24
14	14	a),b),c) illustrates Top view and d),e),f) Side view of the optimized Ni adsorbed geometries at the T _{se} , H and T _w sites respectively. The atoms in orange, blue and	25

		green colour represents the Se, W and Ni atoms respectively.	
15	15	a),b),c) illustrates Top view and d),e),f) Side view of the optimized Fe adsorbed geometries at the T _{Se} , H and T _W sites respectively. The atoms in orange, blue and black colour represents the Se, W and Fe atoms respectively.	26
16	16	a),b),c) illustrates plotted DOS curve, d),e),f) plotted WSe ₂ PDOS and g),h), i) plotted Cu, Ni, Fe PDOS curve for the Cu, Ni and Fe decorated WSe ₂ monolayer respectively.	28
17	17	Charge density diagram for (a)Cu, (b)Ni and (c) Fe decorated onto the WSe ₂ monolayer respectively.	30

List of Symbols, Abbreviations and Nomenclature

S. No.	Acronym/Symbol	Full Form
1	TMDs	Transition Metal Dichalcogenides
2	TM	Transition Metal
3	WSe ₂	Tungsten Diselenide
4	DFT	Density Functional Theory
5	GS	Ground State
6	LDA	Local Density Approximations
7	GGA	Generalised Gradient Approximations
8	PBE	Perdew-Burke-Ernzerhof
9	BFGS	Boryden-Fletcher-Goldfarb-Shanno
10	DOS	Density of States
11	PDOS	Projected Density of States
12	ML	Monolayer
13	E _g	Band-Gap
14	Å	Angstrom
15	eV	electron-volt
16	Ry	Rydberg
17	Se	Selenium
18	W	Tungsten
19	Cu	Copper
20	Fe	Iron
21	Ni	Nickel
22	E _{ad}	Adsorption Energy
23	E _{total}	Total energy of the TM absorbed onto monolayer structure
24	E _{TM}	Total energy of the isolated Transition Metal Atom
25	E _{WSe2}	Total energy of the pristine WSe ₂ monolayer
26	n(r)	Particle Density

27	$V(r)$	Columbic Potential
28	$U[n]$	Interaction Energy
29	$T[n]$	Kinetic Energy
30	X_C	Exchange-Correlational energy
31	Δp	Charge density difference
32	$\mathbf{p}_{\text{total}}$	Charge density of the TM Decorated WSe ₂ monolayer
33	\mathbf{p}_{TM}	Charge density of the isolated Transition Metal Atom
34	$\mathbf{p}_{\text{WSe}_2}$	Charge density of the pristine WSe ₂ monolayer
35	H-site	Hollow Site
36	T _{Se} -site	Top of Selenium Site
37	T _W -site	Top of Tungsten Site

CHAPTER 1

INTRODUCTION

Over the past few years, nanomaterials have revolutionised various scientific fields and industries due to their unique and enhanced properties. Their popularity can be attributed to several compelling reasons, highlighting their unique capabilities and transformative potential in various fields[1-3]. Unlike their bulk counterparts, nanomaterials exhibit exceptional characteristics, making them indispensable in modern technology and innovation. The properties of nanomaterials that enable their widespread use include a high surface area-to-volume ratio, high mechanical strength, exceptional thermal and electrical conductivity, increased chemical reactivity, and unique optical properties[4-6]. These unique characteristics make nanomaterials highly suitable for many practical applications. For example, they can be engineered to deliver drugs to target cells, develop smaller, faster, and more efficient transistors, and enable the creation of flexible and wearable[7-9] electronic devices, which are increasingly in demand for consumer electronics and medical devices, among many other applications[10-12]. Nanomaterials are categorised as 0-D, 1-D, 2-D, and 3-D based on the quantum confinement of electrons, which restricts electron movement within specific dimensions, leading to distinct electronic and optical properties[4, 13-15].

0-D nanomaterials (nanoparticles)-Their properties change as their size approaches the nanoscale, and they show very different optical properties due to quantum effects as they confine electrons at petite sizes[16, 17].

1-D nanomaterials (nanowires/nanotubes)—With a diameter on the nanometre scale, they have two quantum-confined directions for electrical conduction and one unconfined direction, resulting in unique optical, electrical, and mechanical properties[18-21].

2-D nanomaterials (Graphene, MoS₂)- These include thin films, planar quantum wells and super lattices with thickness in the nanoscale range. They have one quantum-confined direction and two unconfined directions for electrical conduction, possessing high electron mobility and flexibility and unique electronic and thermal conductivities due to their planar structure. The transport phenomena in these structures are significantly affected by defects, interfaces, and boundaries on their surface. I chose 2D materials because they offer

unparalleled electronic and thermal conductivity advantages, making them ideal for high-performance applications[21-23].

3-D Nanomaterials- These include bulk nanocrystalline films[24] and nanocomposites[25]. A nanocomposite is a solid material comprising multiple phases, with at least one phase having less than 100 nm dimensions. It typically involves a combination of a bulk matrix and nano-dimensional phases that differ in structure and chemistry from the matrix. Nanocomposites exhibit distinct mechanical, electrical, thermal, optical, electrochemical, or catalytic properties compared to their components. Size thresholds for various effects include <5 nm for catalytic activity and <20 nm for transforming a hard magnetic material into a soft one. Nanocomposites can combine different materials, such as bulk organic materials with organic nanostructures[26], bulk inorganic materials with inorganic ones or a mixture of both[27-29].

In summary, the exceptional properties of nanomaterials, from high surface area to unique optical behaviours, enable a wide range of innovative applications across multiple fields. These materials, whether 0-D, 1-D, 2-D, or 3-D, present unprecedented opportunities for technological applications

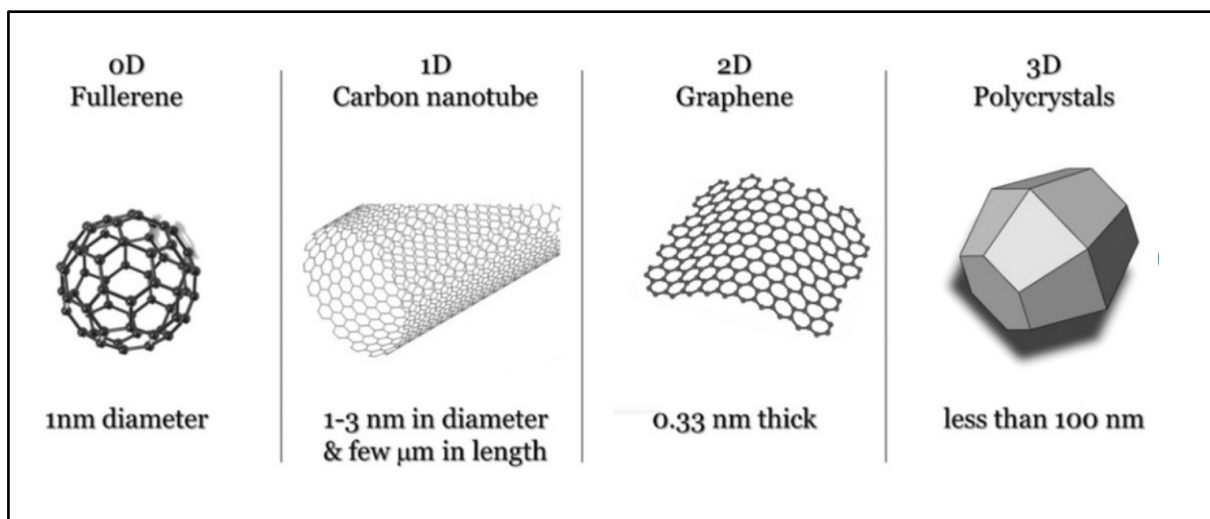


Fig.(1) represents the different types of nanomaterials basis of quantum confinement of electrons

1.1 Two-Dimensional Nanomaterials

Two-dimensional (2D) nanomaterials exhibit extraordinary properties that distinguish them from their bulk counterparts and other nanomaterials[30]. One of their most remarkable features is their high surface-to-volume ratio, which results from their atomic-scale thickness[31]. This unique characteristic offers opportunities for surface interactions, making them highly reactive and facilitating enhanced catalytic activity, gas sensing, and surface

adsorption phenomena[32]. Additionally, the atomically thin nature of 2D materials contributes to exceptional mechanical flexibility and strength, rendering them suitable for applications requiring bendability and resilience, such as flexible electronics, wearable devices, and advanced composite materials[33, 34]. Furthermore, 2D nanomaterials demonstrate intriguing electronic properties, including high carrier mobility, tunable bandgaps, and quantum confinement effects[35]. Graphene, for instance, possesses exceptional electrical conductivity due to its ballistic transport of charge carriers[36]. Transition metal dichalcogenides (TMDs)[37], another class of 2D materials, exhibit distinct bandgap properties that can be tuned by adjusting their thickness, offering opportunities for designing novel electronic and optoelectronic devices. The optical properties of 2D materials are highly tunable, spanning a broad spectrum from the visible to the infrared region, with applications in photodetection, light emission, and optical modulation. Overall, the unique properties of 2D nanomaterials make them up-and-coming candidates for a wide range of technological applications, from electronics and photonics to energy conversion and environmental sensing[38-40]. For my project, I chose transition metal dichalcogenides (TMDs) due to their fascinating electronic and optical properties, which stem from their unique structure, making them particularly suitable for innovative applications in advanced technology.

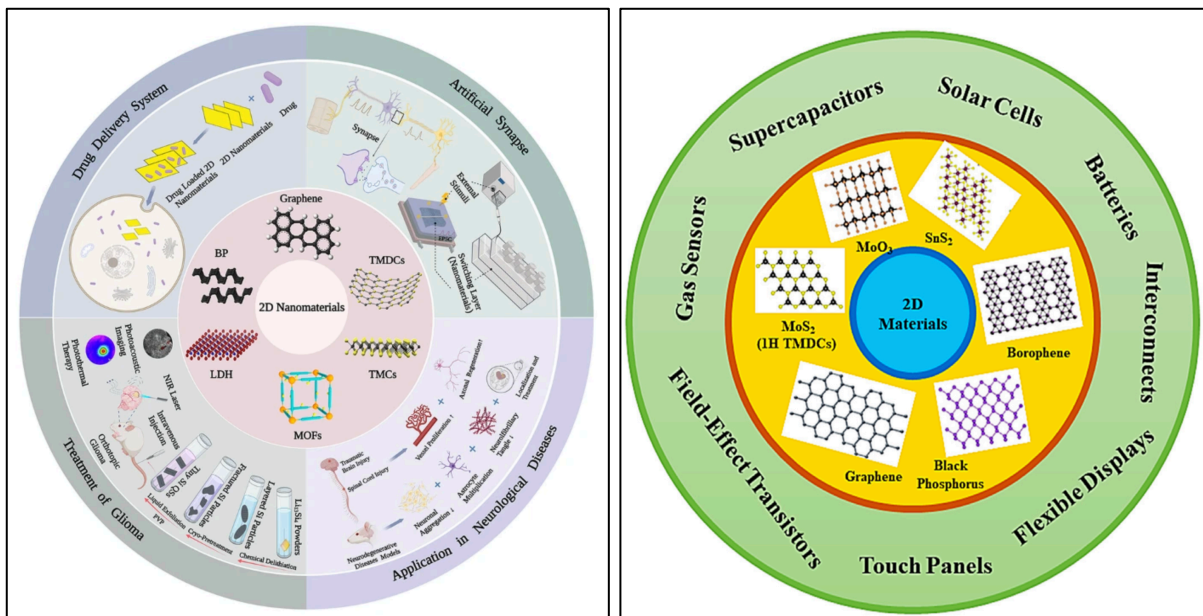


Fig.(2) represents different types of 2D nanomaterials and their applications in various fields.

1.2 Transition Metal Dichalcogenides

Transition metal dichalcogenides (TMDs) are a fascinating class of two-dimensional (2D) materials known for their unique structural and electronic properties, attracting significant

attention in recent years[41, 42]. TMDs consist of layers of transition metal atoms sandwiched between two layers of chalcogen atoms, such as sulphur (S), selenium (Se), or tellurium (Te), forming a hexagonal lattice structure. This layered structure has intriguing electronic properties, making TMDs highly versatile for various applications.

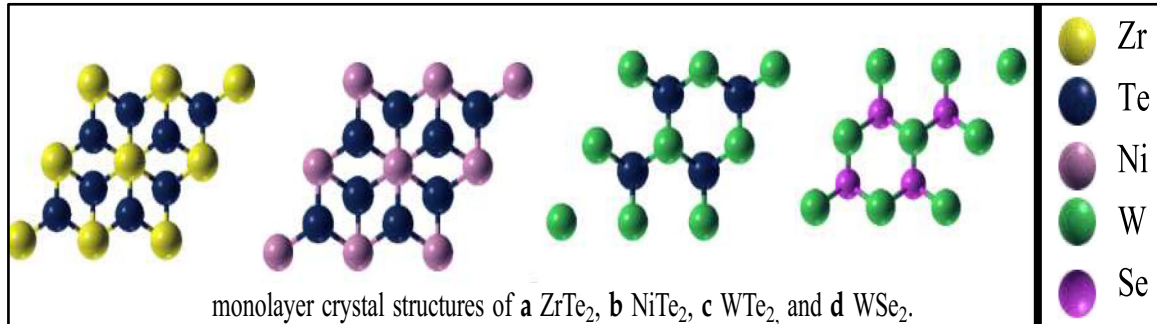


Fig.(3) represents four different Transition Metal dichalcogenides Monolayer(TMD ML)

One of the most widely studied TMDs is molybdenum disulfide (MoS_2)[43], which features a single layer of molybdenum atoms between two sulphur atoms. MoS_2 's structure allows for easy exfoliation into atomically thin layers, imparting remarkable mechanical flexibility and strength, making it suitable for flexible electronics, wearable devices, and strain-sensitive sensors. Other TMDs, such as tungsten disulfide (WS_2)[44] and tungsten diselenide (WSe_2)[45], also garner significant interest due to their distinct properties. WS_2 , with its direct bandgap in the visible range, is ideal for optoelectronic applications like photodetectors, light-emitting diodes (LEDs), and solar cells. WSe_2 , which has an indirect bandgap, offers superior charge carrier mobility, making it ideal for high-speed electronic devices and field-effect transistors[46, 47].

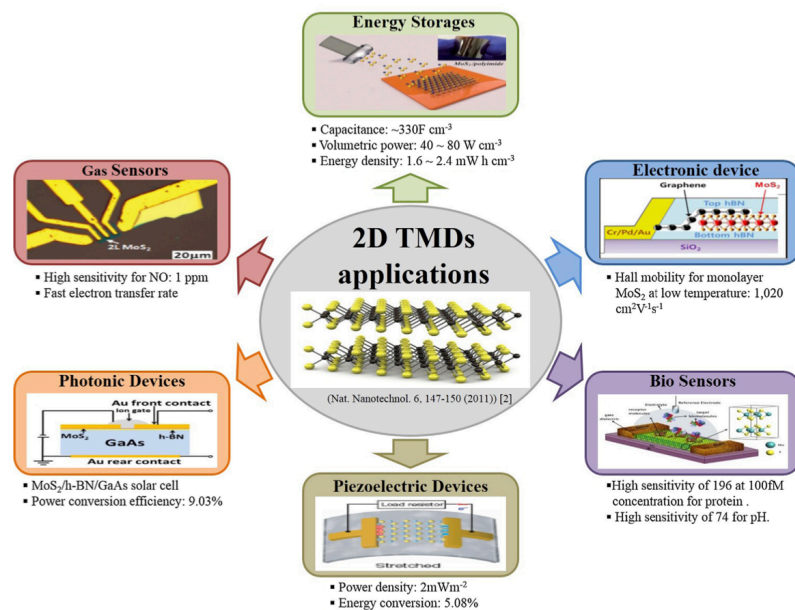


Fig. (4) represents applications of Transition Metal dichalcogenides Monolayer (TMD ML) in various fields.

The unique electronic properties of TMDs arise from their band structure, governed by quantum confinement effects and strong electron-electron interactions in the 2D plane. Unlike bulk materials with continuous electronic states, TMDs exhibit discrete electronic energy levels due to quantum confinement in the out-of-plane direction. Consequently, TMDs are promising candidates for applications in optoelectronics and photonics, making them highly valuable for future technological advancements[48, 49].

1.3 WSe₂ Monolayer

WSe₂, a member of the transition metal dichalcogenides (TMDs) family, features hexagonally arranged tungsten (W) and selenium (Se) atoms within stacked Se-W-Se slabs. The hexagonally arranged W-Se atoms are held together by strong covalent interactions, while the neighbouring Se-W-Se slabs are connected by weak van der Waals forces [49]. As a monolayer, WSe₂ exhibits remarkable properties compared to its bulk form. It is a semiconductor with a direct bandgap of approximately 1.27 eV, enabling efficient light absorption and emission. This makes WSe₂ highly suitable for optoelectronic applications such as photodetectors, light-emitting devices, and solar cells. Additionally, WSe₂ possesses strong spin-orbit coupling and high carrier mobility, facilitating spin manipulation and fast charge transport. Its superior chemical stability and mechanical flexibility further enhance its suitability for reliable, long-term devices operating in harsh environments. These inherent properties position WSe₂ as a promising candidate for a wide range of applications, including optoelectronics, Nano electronics, spintronic, sensors, and photonics, underscoring its potential to revolutionize these fields.

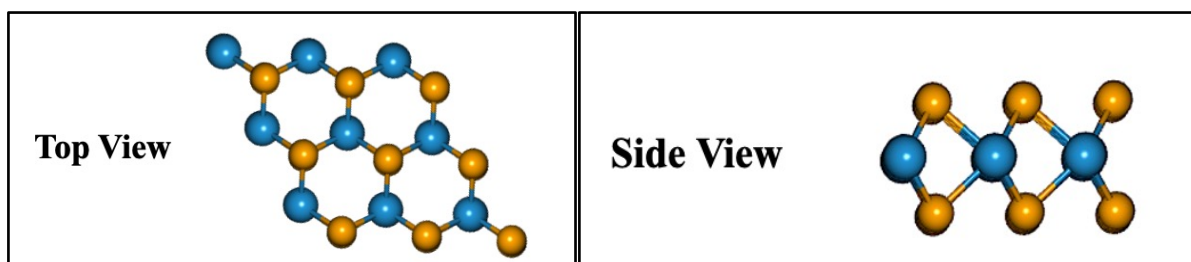


Fig. (5) represents the top view and side view of the WSe₂ Monolayer

Despite its potential, there remains an inevitable need to enhance the electronic, mechanical, optical, and thermal properties of WSe₂ to unlock its applications fully. Enhancing these properties is important to realise the complete potential of WSe₂ monolayers in diverse

technological applications. By improving its performance and functionality, advanced technologies can be developed[50].

1.4 Doping as Strategy

Researchers have increasingly employed doping methods involving 3d transition metal (TM) atoms to enhance the properties of 2D materials. Numerous theoretical studies have demonstrated significant improvements following surface modification with 3d TM atoms. Building on these insights, our study investigates the adsorption of TM atoms such as Cu, Ni, and Fe onto WSe₂ monolayers, focusing on the effects of surface modification on pristine WSe₂[51]. Surface modification presents several advantages, including precise control over doping concentration and distribution without introducing structural defects. Additionally, this method allows for selective functionalization of specific regions within the monolayer, enabling tailored enhancements to its properties[52,53]. The impact of surface modification on WSe₂ monolayers is multifaceted, affecting various aspects of its properties. Firstly, surface doping can substantially alter the material's electrical conductivity, leading to improved carrier mobility and charge transport characteristics. These enhancements are crucial for applications in electronic devices such as transistors and sensors. Moreover, surface modification can influence the mechanical properties of the monolayer, including its flexibility, stiffness, and resistance to deformation[54]. By introducing dopant atoms onto the surface, researchers can modulate interlayer interactions and mechanical stability, enhancing the material's mechanical robustness and durability. Overall, the surface modification of WSe₂ monolayers through 3d TM atom doping offers a versatile approach to fine-tuning the material's properties, positioning it as a promising candidate for advanced applications in electronics, optoelectronics, and beyond.

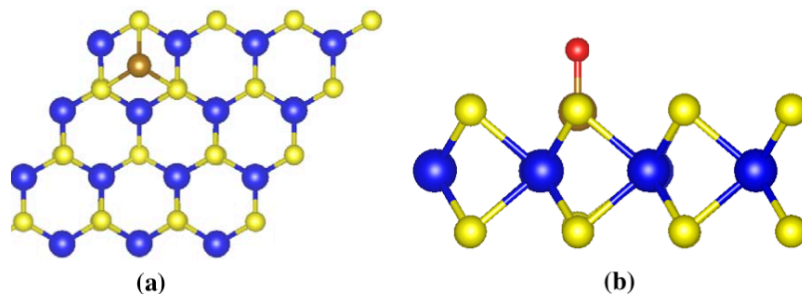


Fig.(6) represents (a) Substitutionally doped Monolayer and (b)Surface-Modification of Monolayer through Adsorption

1.5 Conclusion

In conclusion, nanomaterials have experienced significant advancements in recent years, largely due to their unique properties and transformative potential across a wide range of scientific disciplines and industrial applications. Nanomaterials, which are classified into zero-dimensional (0-D), one-dimensional (1-D), and two-dimensional (2-D) categories based on quantum confinement effects, exhibit exceptional properties that have driven innovation and technological progress. Among these, two-dimensional (2D) materials such as graphene and transition metal dichalcogenides (TMDs) stand out for their high surface area, mechanical flexibility, and remarkable electronic properties[55]. In particular, TMDs like molybdenum disulfide (MoS_2), tungsten disulfide (WS_2), and tungsten diselenide (WSe_2) have garnered significant attention for their diverse applications in fields such as flexible electronics and optoelectronic devices. Our focus on WSe_2 monolayers highlights their exceptional potential in optoelectronics and sensor technology. WSe_2 , with its direct bandgap of approximately 1.27 eV, strong spin-orbit coupling, high carrier mobility, and superior chemical stability, is poised to play a crucial role in developing next-generation devices. These properties enable efficient light absorption and emission, spin manipulation, and fast charge transport, making WSe_2 an ideal candidate for photodetectors, light-emitting devices, solar cells, and spintronic and nanoelectronics applications. To further enhance the properties of TMDs, our exploration of the effects of transition metal atom adsorption using Density Functional Theory (DFT) provides valuable insights. Understanding and manipulating the atomic-scale interactions within these materials can unlock new functionalities and improve performance, paving the way for advanced technologies. This research contributes to the fundamental understanding of TMDs and opens up new avenues for their application in cutting-edge technologies. Overall, nanomaterials, particularly 2D materials, hold immense promise for revolutionizing technology across various sectors. This field's ongoing research and development efforts are crucial for harnessing their full potential. As we continue to explore and innovate, the unique attributes of nanomaterials will undoubtedly lead to ground-breaking advancements, offering solutions to some of the most pressing challenges in modern technology. The future of nanomaterials is bright, and their impact on scientific and industrial progress is poised to be profound and far-reaching.

CHAPTER 2

COMPUTATIONAL METHODOLOGY

2.1 Density Functional Theory

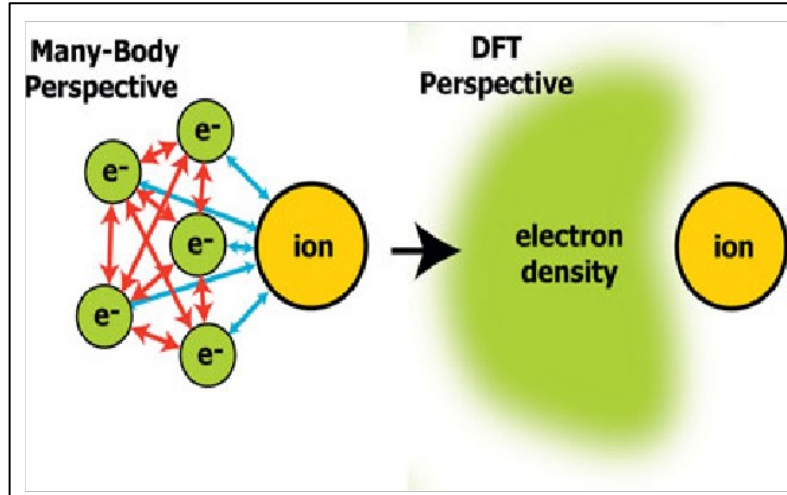


Fig.(7) represents theme of Density Functional Theory

Density Functional Theory (DFT) is a cornerstone in quantum mechanics, offering a robust framework for probing the electronic makeup of atoms, molecules, and solids. Widely embraced for its versatility, DFT is adept at determining molecule binding energies and solids' band structure. Its reach extends beyond traditional quantum realms, finding utility in biology and mineralogy[56]. Moreover, DFT has delved into diverse domains, including superconductivity, laser-induced atomic dynamics, relativistic effects in heavy elements, and the magnetism of alloys. At its core, DFT relies on elementary quantum principles. This framework encapsulates the system's behaviour in its wave function, denoted as Ψ . Focusing on electronic structures, where nuclear influences are captured as a potential $V(r)$ acting on electrons, the Schrödinger equation governs the system. For a lone electron in a given potential, the equation simplifies to Eq. (1).

$$\left(-\frac{\hbar^2}{2m} \nabla^2 + V(r) \right) \psi(r) = E\psi(r) \quad - (1)$$

However, for systems with multiple electrons, such as atoms or molecules, the equation becomes more intricate due to electron-electron interactions, as depicted in Eq. (2), where $U(r_i, r_j)$ represents these interactions[57]. While the kinetic energy operator remains constant across systems, the potential $V(r_i)$ distinguishes between them.

$$\left[\sum_i^N \left(-\frac{\hbar^2 \nabla_i^2}{2m} + V(r_i) \right) + \sum_{i<j} U(r_i, r_j) \right] \psi(r_1, r_2, \dots, r_N) = E \psi(r_1, r_2, \dots, r_N) \quad - (2)$$

Traditionally, solving the Schrödinger equation involves specifying the potential $V(\mathbf{r})$, solving for the wave function Ψ , and deriving observables from it. One crucial observable is the particle density, $n(\mathbf{r})$, expressed in Eq. (3)..

$$n(\mathbf{r}) = N \int d^3r_2 \int d^3r_3 \dots \int d^3r_N \psi^*(\mathbf{r}, r_2, \dots, r_N) \psi(\mathbf{r}, r_2, \dots, r_N) \quad - (3)$$

Various methods, like diagrammatic perturbation theory and configuration interaction (CI) methods, have been devised to tackle the many-body problem posed by the Schrödinger equation. However, these methods prove computationally burdensome for complex systems. For instance, simulating the properties of a 100-atom molecule using full CI or analysing the electronic structure of a semiconductor with Green's functions alone exceeds current computational capacities[58]. For many-electron systems, the equation becomes more complex due to electron-electron interactions. Density functional theory (DFT) offers a versatile approach to electronic structure calculations, recognizing that the potential $V(\mathbf{r})$ is the distinguishing factor in nonrelativistic Coulomb systems. By focusing on universal operators T and U , DFT transforms the many-body problem into a single-body problem, elevating particle density $n(\mathbf{r})$ to a central variable from which all other properties can be derived. This foundational framework underlies the majority of electronic structure computations in physics and chemistry, greatly enhancing our comprehension of materials' electrical, magnetic, and structural characteristics. Despite the conceptual simplicity suggesting that knowledge of $n(\mathbf{r})$ entails understanding the wave function, potential, and other observables, practical implementation of DFT often bypasses explicit consideration of many-body wave functions. While DFT is formally exact, its accuracy in practice hinges on the quality of approximate density functionals. Modern density functionals yield highly precise predictions for various properties of realistic systems, such as molecular bond lengths, solid lattice constants, and molecular energies. However, certain properties, like energy gaps in solids, may exhibit significant deviations. DFT is a potent many-body theory utilizing functionals and their derivatives to tackle the electronic structure conundrum[59]. A functional $F[n]$ is a rule associating a function $n(\mathbf{r})$ with a numerical value.

$$\int d^3r n(\mathbf{r}) = N[n] \quad - (4)$$

In practical Density Functional Theory (DFT), particle number functional and other functionals, such as the Hartree potential V_{Hn} , can be parameter-dependent. The ground-state energy E_V for a given density $n_0(\mathbf{r})$ is determined by minimizing the energy functional $E_V[n]$, which comprises the internal-energy functional $F[n]$ and the potential energy term. $F[n]$ is universal, relying solely on the operators T and U . The cornerstone of DFT is the Hohenberg-Kohn (H-K) theorem, which states that the ground-state wave function Ψ_0 and all observables are unique functionals of the ground-state density $n_0(\mathbf{r})$. This implies that knowing $n_0(\mathbf{r})$ is equivalent to knowing Ψ_0 despite their dimensional differences. The theorem's validity has been confirmed through constrained search and contradiction. Although refined over time with various proofs, representability issues persist particularly the v -representability problem, which concerns determining if a density corresponds to a ground state of a local potential. In practical DFT, one begins with a specified system characterized by a known potential $V(\mathbf{r})$ and reliable approximations for the interaction energy $U[n]$ and kinetic energy $T[n]$ [58]. The objective is to minimize the total energy function. While the N -representability problem has been solved, ensuring any non-negative function can represent a density from an antisymmetric wave function, the v -representability problem remains partially unresolved, especially in continuum systems. Despite these challenges, DFT remains a valuable tool for understanding and predicting the properties of diverse materials and systems.

$$E_v[n]T[n] + U[n] + V[n] = F[n] + V[n] \quad - (5)$$

The electron density, denoted as $n(\mathbf{r})$, is determined through minimization in Density Functional Theory (DFT), yielding the ground-state charge density $n_0(\mathbf{r})$ and ground-state energy $E_V[n_0]$. This density defines the ground-state wave function and informs the entire Hamiltonian and all excited states. DFT enables practical calculations of various physical properties, such as molecular geometries, lattice constants, charge distributions, and energy-related properties like total, dissociation, electron affinities, and ionization energies. These calculations utilize the Hellmann-Feynman theorem to derive forces on atoms from total energy derivatives with respect to nuclear coordinates. However, challenges arise from issues like N - and v -representability and the non-uniqueness of potentials[60]. In spin-DFT or current-DFT, densities do not uniquely specify corresponding potentials, leading to non-uniqueness matters requiring careful consideration. An earlier approximation method, the Thomas-Fermi (TF) approximation, is a foundational approach. It approximates kinetic and interaction energies using local-density approximations (LDA) and assumes the system can be segmented into small cells with constant density and potential. Despite its limitations, such as predicting

molecular instability and inaccuracies due to neglecting correlations and using local approximations, the TF approximation lays the groundwork for more sophisticated methods like orbital-free DFT and modern density functionals. These advancements enhance accuracy in kinetic and exchange-correlation energy calculations, which are crucial for realistic simulations in chemistry and physics. DFT simplifies the treatment of many electron systems by using the total energy as a function of the electron density instead of the wave function. This theoretical framework centres on the electron density, determined by solving Kohn-Sham equations derived from the Hohenberg-Kohn theorems[59,60]. These equations describe non-interacting electrons moving in an effective potential, incorporating contributions from external potentials (e.g., nuclei) and the exchange-correlation functional, representing electron-electron interaction effects. DFT calculations offer insights into material properties such as electronic structure, bonding, energetics, and response properties. Despite its approximations, DFT has become indispensable in theoretical and computational chemistry, physics, and materials science due to its balance of accuracy and computational efficiency[58]. Various software options are available for DFT calculations, including VASP, GPAW, ABINIT, CASTEP, WIEN2k, CP2K, Octopus, SIESTA, Quantum Espresso, and FHI-aims. Quantum Espresso stands out for its versatility and efficiency in ab initio simulations.

2.2 Quantum Espresso

Quantum ESPRESSO is an integrated suite of open-source computer codes designed for electronic structure calculations and material modelling at the nanoscale. To achieve these goals, it utilises density functional theory (DFT), plane waves, and pseudopotentials. The software primarily solves the Kohn-Sham equations, which are derived from DFT. These equations describe non-interacting electrons within an effective potential that accounts for exchange-correlation effects. In Quantum ESPRESSO, electronic wavefunctions are expanded using a plane wave basis set. This approach provides a flexible representation capable of capturing both localised and delocalised electronic states[61]. To simplify electron-nucleus interactions and reduce computational costs, pseudopotentials are employed. These pseudopotentials replace the complex effects of core electrons with smooth potentials that approximate the actual interaction. Brillouin zone integrations are a critical aspect of Quantum ESPRESSO, and efficient algorithms like the Monkhorst-Pack scheme are used to ensure precise electronic property calculations. The self-consistent field (SCF) procedure is employed to iteratively update the electron density until convergence is achieved, ensuring both accuracy and stability in the results. Quantum ESPRESSO enables detailed and reliable modelling of

material properties at the atomic and electronic levels through these sophisticated techniques. Quantum ESPRESSO is a versatile and powerful tool for computational materials science. It offers a broad array of functionalities for simulating and understanding the properties of materials at the atomic scale. Its open-source nature encourages collaboration and continuous development, making it a valuable resource for researchers worldwide[62].



Fig.(8) represents LOGO of Quantum Espresso

2.3 Exchange-Correlation Energy

The exchange-correlation (Xc) energy is a crucial aspect of Density Functional Theory (DFT), essential for accurately handling the kinetic and interaction energies among interacting electrons[63]. The kinetic-energy functional, denoted as $T[n]$, can be split into two components: the kinetic energy of noninteracting electrons, $T_s[n]$, and the remaining part, which signifies the correlation, $T_c[n]$:

$$T[n]=T_s[n]+T_c[n] \quad - (6)$$

The kinetic energy of noninteracting particles, $T_s[n]$, is not precisely known as a density functional, but it can be represented in terms of single-particle orbitals, $\phi_i(r)$, of a noninteracting system:

$$T_s[n] = -\frac{\hbar^2}{2m} \sum_i^N \int d^3r \phi_i^*(r) \nabla^2 \phi_i(r) \quad - (7)$$

These orbitals, $\phi_i(r)$, are functionals of the density n , rendering T_s an implicit density functional.

The exact energy functional can be expressed as:

$$E[n] = T[n] + U[n] + V[n] = T_s[\{\phi_i[n]\}] + U_H[n] + E_{xc}[n] + V[n] \quad - (8)$$

Here, $U_H[n]$ represents the Hartree energy, and $E_{xc}[n]$ denotes the exchange-correlation energy. The E_{xc} term accounts for the differences $T-T_s$ (i.e., T_c) and $U-U_H$, thus ensuring formal exactness. While E_{xc} is assured by the Hohenberg-Kohn (HK) theorem to be a density functional, its exact form remains unknown. The exchange-correlation energy E_{xc} is often decomposed into:

$$E_{xc}=E_x+E_c \quad -(9)$$

Where E_x represents the exchange energy originating from the Pauli exclusion principle, and E_c stands for the correlation energy[64]. The exchange energy, E_x , can be explicitly formulated in terms of the single-particle orbitals as:

$$E_x[\{\phi_i[n]\}] = -\frac{q^2}{2} \sum_{jk} \int d^3r \int d^3r' \frac{\phi_j^*(r)\phi_k^*(r')\phi_j(r')\phi_k(r)}{|r-r'|} \quad (10)$$

known as the Fock term. However, no general exact expression for E_x or E_c in terms of the density is known.

2.3.1 Generalized Gradient Approximation

Generalized Gradient Approximation (GGA) is a widely used approach within Density Functional Theory (DFT) to improve the accuracy of the exchange-correlation energy function. In DFT, the exchange-correlation function is crucial because it accounts for the complex many-body interactions among electrons, encompassing exchange interactions (arising from the Pauli exclusion principle) and correlation interactions (arising from electron-electron repulsion). The fundamental idea behind DFT is to reduce the problem of solving the many-electron Schrödinger equation to a more manageable problem involving electron density, $\rho(r)$, instead of the many-electron wave function, Ψ [65]. The fundamental quantity in DFT is the total energy as a function of the electron density, including kinetic energy, external potential energy, and the exchange-correlation energy.

Before GGA, local density approximation (LDA) was the primary method for approximating the exchange-correlation function. Some of the most widely used GGA functionals include:

1. Perdew Burke Ernzerhof (PBE)- One of the most popular GGA functionals, known for its robustness and broad applicability across various systems. The PBE functional incorporates physically motivated constraints to improve the accuracy of both exchange and correlation terms.

2. Beckee(B88) and Lee Yang Parr(LYP) - These functionals are often used in combination, B88 for exchange and LYP for correlation, forming the BLYP functional. They are particularly popular in quantum chemistry for molecular systems

3. PW91- It was developed by Perdew and Wang, another well-regarded GGA functional, especially in the field of solid-state physics.

ADVANTAGE OF GGA-By incorporating the electron density gradient, GGA provides a more accurate description of exchange-correlation effects compared to LDA, particularly for

systems with rapidly varying densities. GGA functionals apply to various materials, from simple metals to complex molecules and surfaces.

DISADVANTAGE OF GGA- GGA can sometimes under bind (underestimate bond strengths) in specific systems, leading to slightly too long bond lengths or over bind in others. GA, like LDA, generally fails to accurately describe long-range van der Waals interactions because these are inherently non-local effects.

The Generalized Gradient Approximation (GGA) represents a significant step forward in the accuracy of DFT calculations by incorporating information about the electron density gradient. While it addresses some of the limitations of LDA and provides better results for many systems, it still has limitations, particularly with non-local interactions. Nevertheless, GGA remains a cornerstone of modern computational materials science and quantum chemistry, striking a balance between computational efficiency and accuracy.

2.4 Convergence Tests

Convergence lies at the heart of Density Functional Theory (DFT) calculations, where obtaining an accurate ground-state electron density involves solving complex mathematical equations through iterative numerical approximations. These approximations, crucial for computational feasibility, aim to approach the exact solution by allocating more computational resources. This iterative process, termed convergence, ensures that a "well-converged" calculation closely approximates the true solution of the DFT problem for a specific exchange-correlation function. Transitioning from the familiar three-dimensional physical space to reciprocal space, a fundamental concept in solid-state physics, is pivotal in understanding DFT calculations. Reciprocal space, represented by k vectors, introduces the Brillouin zone (BZ), which is essential in materials' band theory. Within the BZ, points like the Gamma point, where k equals 0, hold particular significance. This continuous shift between physical and reciprocal space highlights the interconnectedness of concepts in practical DFT applications. Efficiently evaluating integrals, a demanding aspect of DFT calculations, led to the development of methods like the Monkhorst-Pack scheme in 1976[66]. This approach, widely adopted in DFT packages, allows selecting k points based on predetermined criteria, typically the desired number of k points in each reciprocal space direction. However, determining the optimal number of k points involves careful consideration, particularly for calculations involving supercells with uniform lattice vectors. Convergence tests play a critical role in ensuring the accuracy and reliability of DFT simulations. Specifically, cut-off energy and K-point convergence tests are essential. Cut-off energy determines the maximum energy of plane waves

included in the basis set, affecting the accuracy of electronic wave function representations. Similarly, K-point convergence involves discretely sampling the Brillouin zone to assess how the density of K-points affects calculation accuracy. These convergence tests, by examining key properties or observables, ascertain the appropriate parameters for accurate and reliable DFT simulations. Ultimately, conducting these tests instils confidence in the computational model's predictive capabilities, reinforcing the credibility of the obtained results.

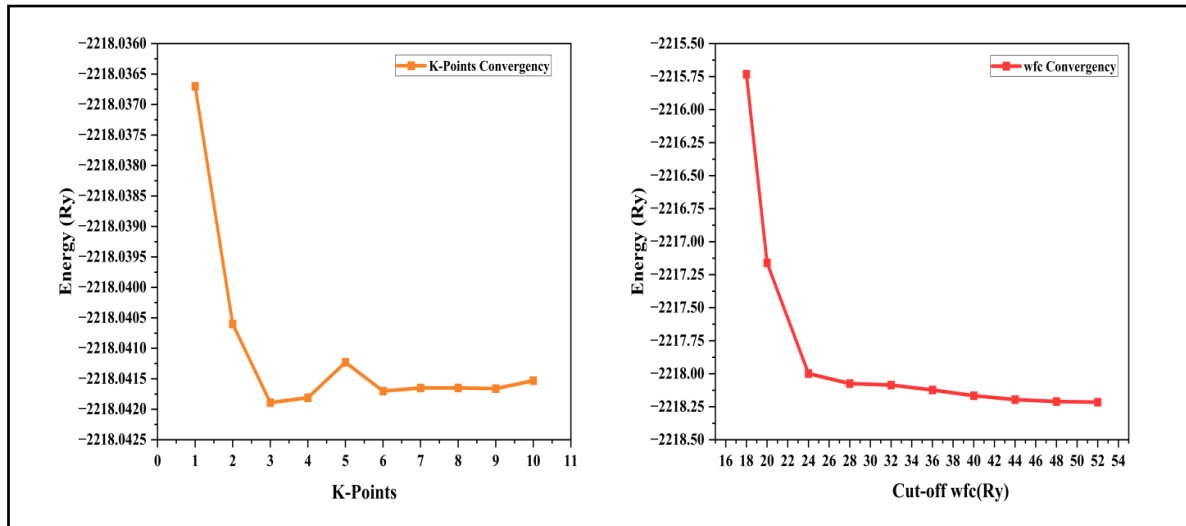


Fig. (9) Curves representing the variation in the ground state energy with (A) K- points and (B) cut-off energy respectively.

2.5 Pseudopotentials:

The above discussion highlights the need for significant energy cut-offs in DFT calculations to capture plane waves with short wavelength oscillations in real space. This requirement poses computational challenges, particularly for core electrons in atoms, which exhibit wave functions with such oscillations. However, core electrons are less significant in defining chemical bonding and material properties than valence electrons. To address this, methods have been developed to approximate core electron properties, thereby reducing computational demands. A primary method to simplify calculations involving core electrons is using pseudopotentials. Pseudopotentials replace the electron density from selected core electrons with a smoothed density that retains the actual ion core's critical physical and mathematical characteristics. This approach, known as the frozen core approximation, fixes the properties of core electrons in subsequent calculations[67]. These calculations, termed frozen core methods, are more common than all-electron calculations, which do not use a frozen core. Typically, a pseudopotential is created for an isolated atom of a specific element and can be used in various chemical environments without further adjustments. Most modern DFT codes provide a library of pseudopotentials for elements across the periodic table. The characteristics of a

pseudopotential determine the minimum energy cut-off required for calculations involving atoms associated with it. Pseudopotentials that require high cut-off energies are called hard pseudopotentials, while those needing lower cut-off energies are termed soft pseudopotentials, which offer greater computational efficiency[68]. A well-known method for defining pseudopotentials is based on Vanderbilt's work, leading to the development of ultrasoft pseudopotentials (USPPs). Although USPPs have lower cut-off energy requirements, they require the specification of several empirical parameters for each atom. Another approach addressing some limitations of USPPs is the projector augmented-wave (PAW) method. Comparisons between USPP, PAW, and all-electron calculations for various systems indicate that well-constructed USPPs and the PAW method yield results nearly identical to those of all-electron calculations in many cases

2.5.1 Ultrasoft Pseudopotentials (USPP):

Ultrasoft pseudopotentials (USPPs) are utilized in Density Functional Theory (DFT) calculations to model the interactions between valence electrons and atomic nuclei. Unlike norm-conserving pseudopotentials, USPPs are designed to be more adaptable and smoother, facilitating a more efficient representation of electron wavefunctions. This is achieved by relaxing the stringent requirement for pseudopotentials to be strictly local, allowing USPPs to provide a smoother potential that more accurately represents the actual electron-nucleus interaction[68]. USPPs are especially beneficial for modelling transition metals and other heavy elements with significant electron-electron correlations.

2.6 Broyden-Fletcher-Goldfarb-Shanno (BFGS) Scheme

The Broyden-Fletcher-Goldfarb-Shanno (BFGS) algorithm is a commonly employed method in Density Functional Theory (DFT) for optimizing the geometry of molecular and solid-state systems. It is part of the quasi-Newton family of methods and is an iterative optimization technique designed to find the minimum of a function, specifically the total energy of the system, in DFT calculations. In the context of DFT, the total energy depends on the atomic positions. The objective of geometry optimization is to identify the atomic arrangement that minimizes this total energy, corresponding to the system's most stable configuration. The BFGS algorithm accomplishes this by iteratively adjusting the atomic positions until the minimum energy configuration is achieved[69]. The BFGS algorithm approximates the Hessian matrix, which represents the second derivatives of the energy with respect to atomic positions. Utilizing this approximation, the algorithm determines the step size and direction to move the system towards the minimum energy configuration. During each iteration, the BFGS

algorithm updates the Hessian matrix approximation based on the changes in the energy gradients with respect to the atomic positions. One significant advantage of the BFGS algorithm is its efficiency in reducing the number of energy evaluations needed to reach the minimum energy configuration. This efficiency is crucial in DFT calculations, where energy evaluations can be computationally intensive. By iteratively updating the atomic positions using effective approximations of the Hessian matrix, the BFGS algorithm facilitates rapid convergence to the minimum energy configuration, making it a favoured choice for geometry optimization in DFT calculations[70].

2.7 Computational Framework

First-principles calculations within Density Functional Theory (DFT) were performed using the QUANTUM ESPRESSO package to study the adsorption of transition metal (TM) atoms on a monolayer surface. The Perdew-Burke-Ernzerhof (PBE) formulation of the Generalized Gradient Approximation (GGA) was employed to model the exchange-correlation function, ensuring an accurate depiction of electronic interactions. These calculations used a plane wave basis set combined with ultrasoft pseudopotentials to represent the electronic wave functions and electron-ion interactions, respectively. Comprehensive convergence tests for cut-off energy and K-points were conducted to ensure reliable results. The Monk horst-Pack scheme with a 7x7x1 K-point mesh and a cut-off energy of 35 Ry was selected for the self-consistent calculations. Structural optimizations were carried out using the Broyden-Fletcher-Goldfarb-Shanno (BFGS) method until the forces on each atom were reduced to less than 10^{-3} Ry/Bohr. A 3x3 supercell consisting of 18 selenium atoms and nine tungsten atoms was constructed to investigate the adsorption of TM atoms on the monolayer surface. A 10 Å vacuum layer was included along the z-direction to prevent interactions between adjacent periodic images, with the TM atom positioned at a distance from the surface. The main objective of these calculations was to explore the stability of the monolayer upon TM atom adsorption and to identify the most favourable adsorption sites on the interface. By systematically analysing various configurations and evaluating their relative energies, insights into the adsorption behaviour and stability of the monolayer-TM atom system were obtained. The relative stabilities of these configurations were measured by their adsorption energy E_{ad} , defined as:

$$E_{ad} = E_{total} - (E_{TM} + E_{WSe_2}) \quad - (11)$$

Where E_{WSe_2} , E_{TM} , and E_{total} represent the total energies of the pristine WSe₂ monolayer, isolated TM atoms, and TM metal adsorbed onto the WSe₂ monolayer structure, respectively.

Equation (2) was used to calculate the charge density difference(Δp), to determine the charge gain and loss upon adsorption of TM atoms onto WSe₂ monolayer.

$$\Delta p = p_{total} - (p_{TM} + p_{WSe_2}) \quad - (12)$$

where p_{WSe_2} , p_{TM} , and p_{total} represent the charge density of the pristine WSe₂ monolayer, isolated TM atom, and TM atom decorated WSe₂ monolayer structure, respectively.

2.8 Outline of the Thesis

To elucidate the entire process, we constructed a model of the tungsten diselenide monolayer using a 3 x 3 supercell. Next, we conducted self-consistent field (SCF) calculations with varying cut-off energies and sets of K points to identify the energy configuration where the system was most stable. This convergence test enabled us to determine the optimal cut-off energy and set of K points required for stability. Following the convergence test, the geometry was optimized using VC-relax calculations, where forces were applied to the monolayer's atoms until the system reached its minimum energy state. The optimized monolayer structure introduced transition metal (TM) atoms at various heights and sites. The geometry of the TM-decorated WSe₂ monolayer was then optimized to achieve the most stable configurations. Subsequently, calculations were performed for isolated TM atoms to determine their energy, along with calculations for the pristine monolayer and the TM-adsorbed monolayer system. These energy values allowed us to calculate the energy required for the monolayer to absorb the TM atoms, revealing whether the absorption process was endothermic or exothermic, spontaneous or non-spontaneous. To investigate the electronic properties of the system, we conducted density of states (DOS) calculations for the WSe₂ monolayer structure, isolated TM atoms, and TM-decorated monolayers. By analysing the change in Fermi levels upon absorption and examining the density of electronic states in the conduction and valence bands, insights were gained into the system's electronic behaviour. Additionally, the system's magnetic properties were analysed by evaluating the symmetry of the up and down spin states through DOS plots, determining whether the system exhibited paramagnetic, diamagnetic, or ferromagnetic behaviour to understand better the system's orbital contributions and hybridization, projected density of states (PDOS) calculations were performed for isolated TM atoms, the WSe₂ monolayer, and the TM-decorated WSe₂ monolayer. Furthermore, charge transfer analysis was conducted using data files, enabling the visualization of the charge density distribution in the TM-decorated WSe₂ monolayer. In summary, this comprehensive approach allowed us to systematically investigate the structural, energetic, and electronic properties of

TM-decorated WSe₂ monolayers, providing valuable insights into their behaviour and potential applications.

CHAPTER 3

RESULTS AND DISCUSSION

3.1 Structure and Electronic properties analysis of WSe₂ Monolayer

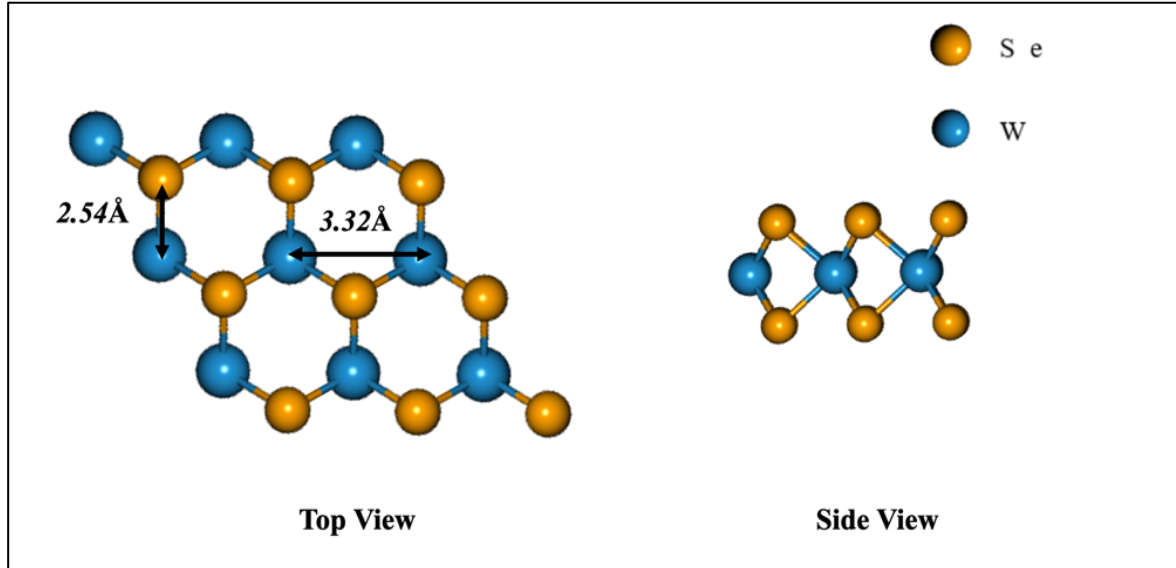


Fig.(10) (a)Top and (b) Side view of the optimized pristine WSe₂ structure respectively. The blue and orange coloured atoms represent the W and Se atoms respectively.

The WSe₂ monolayer, a two-dimensional material, features a hexagonal lattice structure with lattice parameters $a = 9.8646 \text{ \AA}$ and $c = 23.3411 \text{ \AA}$. Each tungsten (W) atom is connected to six selenium (Se) atoms, while each Se atom is bonded to three W atoms. Upon optimization, the stable bond lengths between W-Se, nearest W-W, and Se-Se atoms were determined to be 2.54 \AA and 3.32 \AA , respectively. The optimization process in Density Functional Theory (DFT) minimizes the total system energy, ensuring the structure achieves its most stable state according to quantum mechanical principles. This process establishes equilibrium positions where atomic forces balance, providing an accurate representation of the ground-state structure, which is crucial for making reliable predictions of material properties. This optimized structure, depicted in Fig.(10), shows the arrangement of atoms in the pristine WSe₂ monolayer, with Se atoms represented in blue and W atoms in orange. The electronic properties of the WSe₂ monolayer were analysed through Density of States (DOS) and Projected Density of States (PDOS) calculations. DOS measures the number of electronic states at a specific energy level, adjusted by the fraction of the total electron density within a specified volume surrounding a nucleus. The DOS curve, shown in Fig.(11)a), indicates the absence of electronic states near the Fermi level, with a calculated band gap of approximately 1.27 eV . This suggests that the

WSe₂ monolayer acts as a semiconductor with a band gap that reflects its electronic properties. Additionally, the symmetric nature of the up and down spin curves in the DOS plot confirms a zero magnetic moment per atom, establishing the paramagnetic behaviour of the WSe₂ monolayer. Further insights into the electronic structure were obtained from the PDOS curve, illustrated in Fig.(11)b). The PDOS analysis reveals strong hybridization between the d orbitals of W atoms and the p orbitals of Se atoms. This hybridization is responsible for the covalent interactions between neighbouring atoms within the material, contributing to its stability and electronic properties. The observed hybridization corroborates previous theoretical works, supporting the findings reported in existing literature. The analysis of the structural and electronic properties of the pristine WSe₂ monolayer reveals its hexagonal lattice structure and stable bond lengths. It behaves as a semiconductor with a calculated band gap and exhibits paramagnetic characteristics. The strong hybridization between atomic orbitals leads to covalent interactions within the material, highlighting its stability and electronic properties. These insights enhance our understanding of the WSe₂ monolayer's attributes and provide a foundation for future materials science and nanotechnology research and applications.

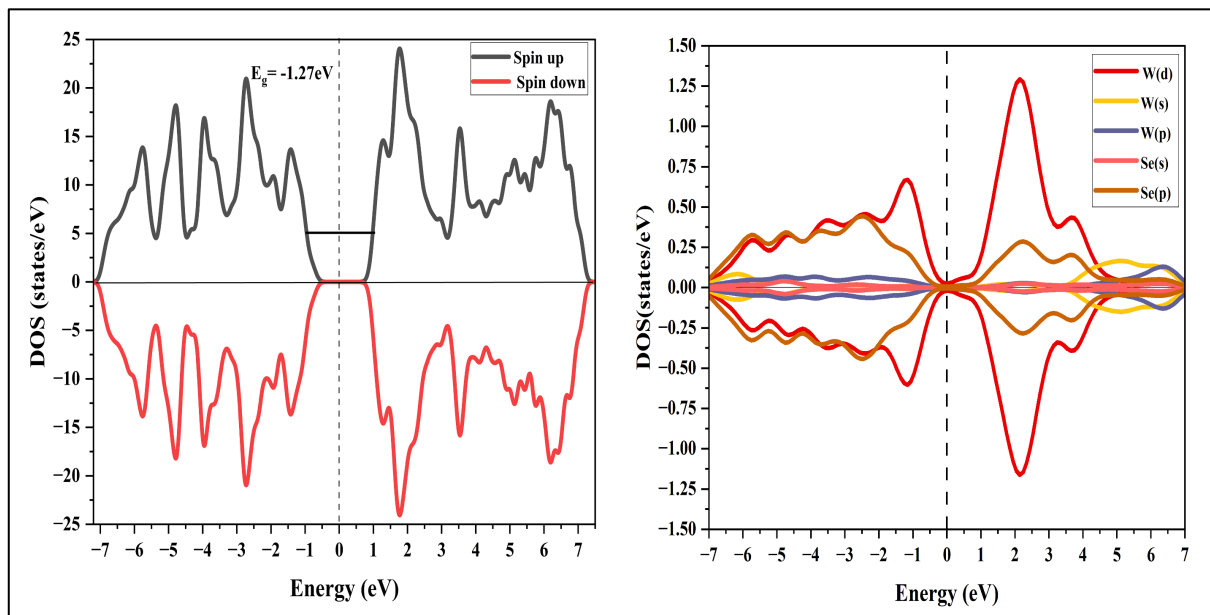


Fig.(11) Plotted a) DOS and b) PDOS for the pristine WSe₂ monolayer respectively.

3.2 Adsorption of TM atoms onto pristine WSe₂ monolayer

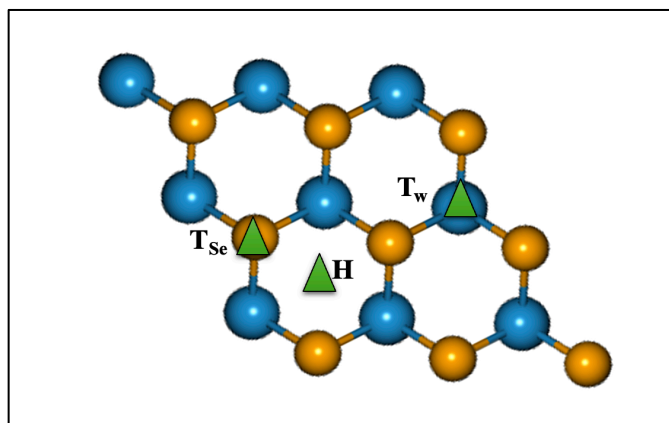


Fig.(12) illustrates the H, T_w, and T_{Se} adsorption sites selected for the adsorption of TM atoms onto WSe₂ monolayers, respectively.

To explore how surface modification by transition metal (TM) atoms such as Cu, Fe, and Ni affects the WSe₂ monolayer, we conducted an adsorption study focusing on three potential adsorption sites labelled H, T_w, and T_{Se}. In the H-site configuration, TM atoms were adsorbed above the centre of the hexagonal ring. In contrast, in the T_w-site and T_{Se}-site configurations, TM atoms were positioned above the W and Se atoms, respectively, as illustrated in Fig.(12). We obtained vital parameters such as adsorption energies and distances through structural optimization to characterize the adsorption process. Adsorption energies were calculated to quantify the interaction strength between the TM atoms and the WSe₂ monolayer, helping to identify the most stable adsorption configurations. Using equation(11), we computed adsorption energies for various configurations presented in Table(1). These energies offer valuable insights into the energetics of TM atom adsorption on the WSe₂ monolayer, highlighting the stability of different configurations. By analysing these energies, we can determine which adsorption sites and configurations are energetically favoured, guiding our understanding of the adsorption process and informing potential applications of TM-modified WSe₂ monolayers. Additionally, adsorption distances, representing the separation between the TM atoms and the WSe₂ monolayer surface upon adsorption, provide crucial information on the spatial arrangement and proximity of the TM atoms to the monolayer. These distances can affect the electronic and structural properties of the modified material, influencing its behaviour and performance in various applications. By systematically investigating adsorption energies and distances for different TM atoms and adsorption sites, we aim to understand the interaction between TM atom adsorption and the properties of the WSe₂ monolayer. This understanding is essential for leveraging the potential of TM-modified WSe₂ monolayers in various technological and scientific fields, including catalysis, sensing, and optoelectronic devices.

3.2.1 Structure and Adsorption Analysis of Cu Atom onto Pristine WSe₂ Monolayer

This section analyses the interaction between a copper (Cu) atom and a tungsten diselenide (WSe₂) monolayer. Using density functional theory (DFT), we initially optimized various geometries for the adsorption study. The optimization process revealed significant structural deformations upon Cu adsorption, indicating substantial changes in bond lengths and the overall geometry of the WSe₂ monolayer. This optimized structure is depicted in Fig(13). Upon examining the optimized WSe₂ structure, we found that Cu atoms adsorb at three distinct sites, the H-site, T_{Se}-site, and T_W-site. The bond lengths between tungsten and selenium atoms (W-Se) were initially measured at 2.540 Å in the pristine monolayer. However, these varied to 2.549 Å, 2.546 Å, and 2.554 Å upon Cu adsorption at the H-site, T_{Se}-site, and T_W-site, respectively. These variations suggest an expansion of the hexagonal ring structure to accommodate the Cu atom, indicating that the monolayer undergoes structural changes to facilitate Cu adsorption. Adsorption energies were calculated for each site, which quantified the strength of the interaction between the Cu atom and the WSe₂ monolayer. The positive values of the adsorption energies indicate that the adsorption process is endothermic, non-spontaneous, and energetically unfavourable.

Table(1): Adsorption sites, adsorption energy(eV), adsorption height (Å) for the optimized Cu, Ni and Fe decorated WSe₂ monolayer respectively.

TM	Adsorption Sites	Adsorption energy (eV)	Adsorption height (Å)
Cu	T _W	3.05	3.15
	T _{Se}	3.40	2.35
	H	3.10	2.51
Ni	T _W	-4.72	2.63
	T _{Se}	-3.26	2.10
	H	-4.14	2.15
Fe	T _W	-0.85	2.61
	T _{Se}	-1.33	2.15
	H	-4.37	2.16

Specifically, the Cu atom adsorbs at distances of 3.15 Å, 2.35 Å, and 2.51 Å from the WSe₂ monolayer at the H-site, T_{Se}-site, and T_W-site, with corresponding adsorption energies of 3.05 eV, 3.40 eV, and 3.10 eV, respectively. This suggests that, among the three sites, the Cu atom

prefers adsorption at the top of the W site (T_W -site) based on energy minimization principles. To further understand the adsorption characteristics, the atomic radii of the Cu and W atoms, which are 1.45 Å and 1.93 Å respectively, were considered. The calculated sum of the atomic radii for the W-Cu interaction is 3.38 Å. Comparing this value to the actual adsorption distances, it was found that the computed sum is larger than the adsorption distances for the most stable adsorption configurations. This discrepancy indicates the formation of covalent bonds between the Cu atom and the WSe₂ monolayer, leading to the classification of the adsorption process as chemisorption. The high adsorption energy observed is consistent with the formation of strong covalent bonds, suggesting a robust interaction between the Cu atom and the WSe₂ monolayer.

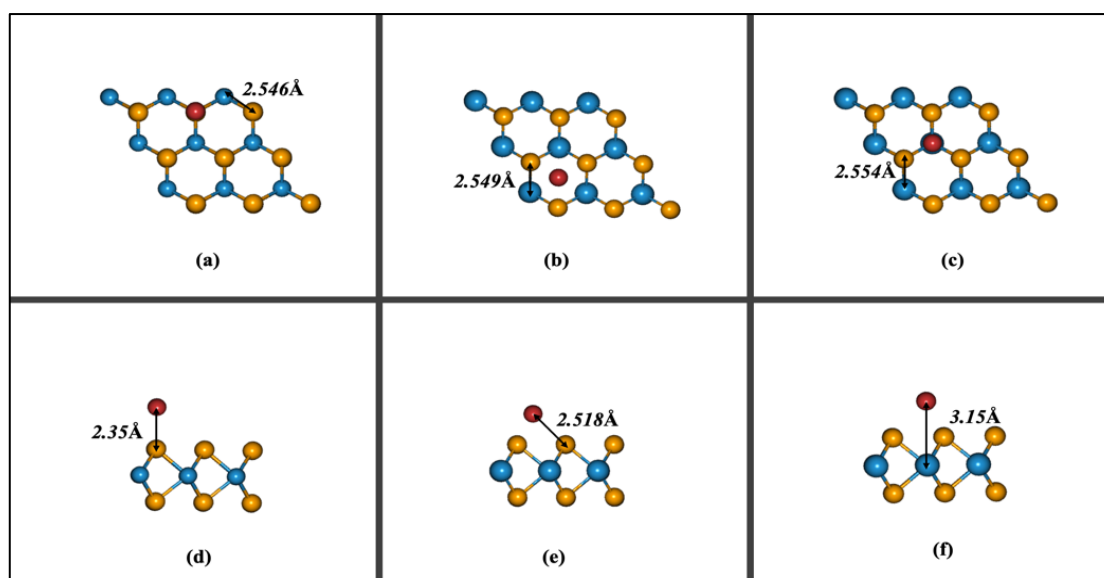


Fig. (13) (a), (b),(c) illustrates the Top view and (d),(e),(f) Side view of the optimized Cu adsorbed geometries at the T_{Se} , H, and T_W sites. The orange, blue, and red atoms represent the Se, W, and Cu atoms, respectively.

3.2.2 Structure and Adsorption Analysis of Ni Atom onto Pristine WSe₂ Monolayer

To investigate the adsorption of a Ni atom onto a WSe₂ monolayer, we fully optimized the initial geometries for the adsorption study. Post-optimization, it was observed that the WSe₂ monolayer deformed to incorporate the Ni atom. The W-Se bond lengths increased from an initial 2.540 Å to 2.542 Å, 2.687 Å, and 2.551 Å upon Ni adsorption at the Se, H, and W sites, respectively, as shown in Fig.(14). The calculated adsorption energies revealed that the Ni atom adsorbs at the Se, H, and W sites with energies of -3.26 eV, -4.14 eV, and -4.72 eV,

respectively. These negative values indicate that the adsorption process is exothermic and energetically favourable.

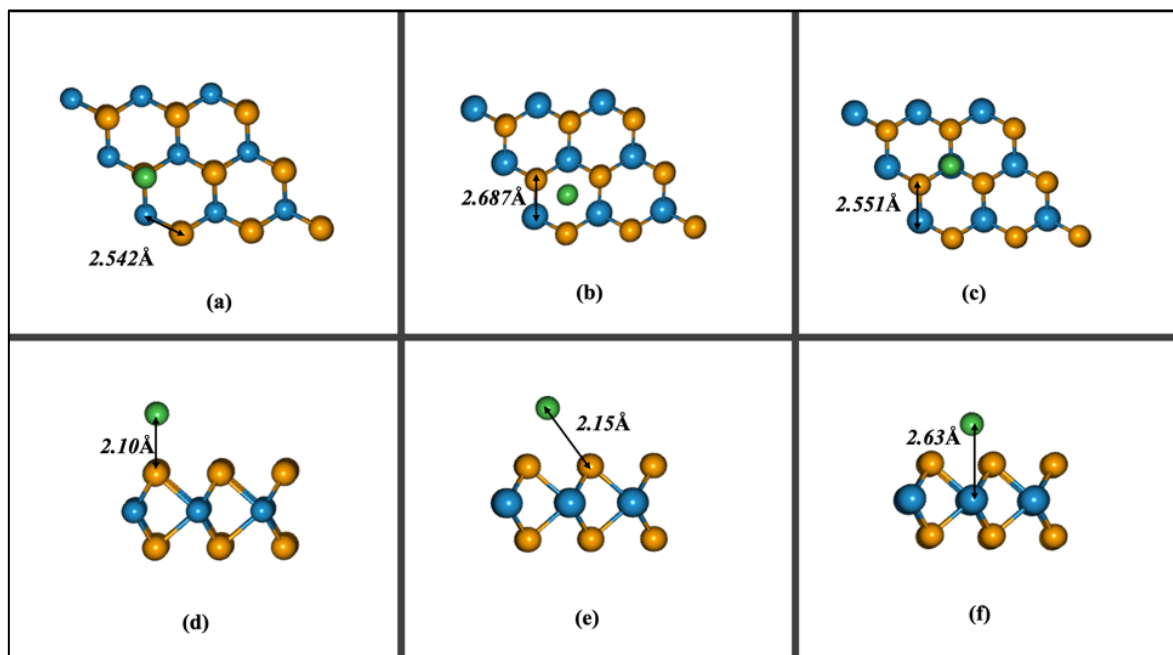


Fig.(14) a),b),c) illustrates Top view and d),e),f) Side view of the optimized Ni adsorbed geometries at the T_{Se} , H, and T_W sites. The orange, blue, and green atoms represent the Se, W, and Ni atoms, respectively.

Energy minimization identified the most stable adsorption configurations, with the Ni atom adsorbing at a height of 2.63 Å above the W site. The significant adsorption energy and minimal adsorption height for the most stable configurations suggest strong covalent bonding between the Ni atom and the WSe₂ monolayer. This strong covalent interaction accounts for the high adsorption energy observed during Ni atom adsorption.

3.2.3 Structure and Adsorption Analysis of Fe Atom onto Pristine WSe₂ Monolayer

The adsorption of a Fe atom onto a WSe₂ monolayer was examined by evaluating different orientations of the Fe atom at the W, Se, and H sites. After optimization, it was found that the W-Se bond lengths varied significantly from their initial values. Specifically, the W-Se bond lengths changed from 2.540 Å to 2.15 Å, 2.16 Å, and 2.61 Å when Fe was adsorbed at the Se, H, and W sites, respectively, as illustrated in Fig.(15). The adsorption energies calculated for Fe at the Se, H, and W sites were -1.33 eV, -4.37 eV, and -0.83 eV, respectively. These negative values indicate that the adsorption process is exothermic and energetically favourable. Energy minimization revealed that the most stable adsorption configuration was with the Fe atom at a height of 2.16 Å at the H site. The significant adsorption energy and short adsorption height for this configuration suggest strong covalent bonding between the Fe atom and the WSe₂

monolayer, which accounts for the high adsorption energy observed. The study also explored the adsorption of transition metal (TM) atoms Cu, Ni, and Fe onto a pristine WSe₂ monolayer. By calculating the adsorption energies and distances, the interaction strength and stability of the adsorbed configurations were understood. The adsorption of Cu, Ni, and Fe atoms led to the deformation of the WSe₂ monolayer, causing notable changes in bond lengths and overall structure. The adsorption energies indicated that Cu adsorption is endothermic and energetically unfavourable, whereas Ni and Fe adsorption is exothermic and energetically favourable. The strong covalent bonding between the TM atoms and the WSe₂ monolayer resulted in high adsorption energies in the most stable configurations. This detailed analysis of optimized structures and adsorption energies offers valuable insights into the interaction mechanisms and stability of TM-decorated WSe₂ monolayers.

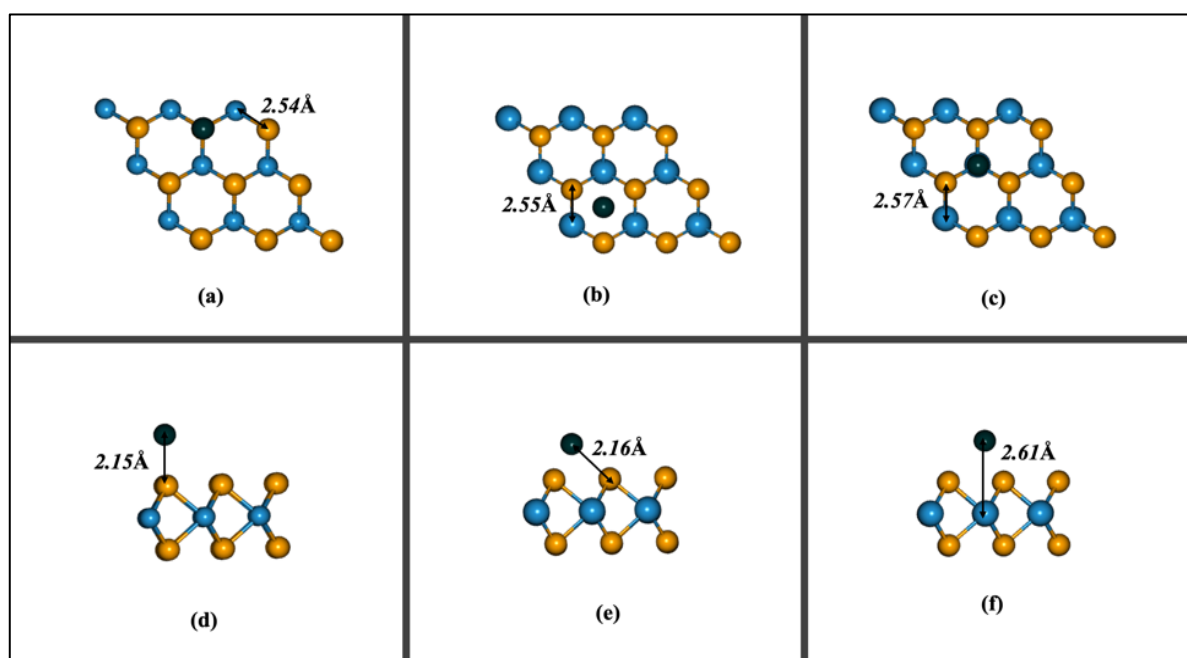


Fig. (15) a),b),c) illustrates Top view and d),e),f) Side view of the optimized Fe adsorbed geometries at the T_{Se}, H and T_w sites respectively. The atoms in orange, blue and black colour represents the Se, W and Fe atoms respectively.

3.2.4 Effect of Cu, Ni, and Fe Adsorption on the Electronic Properties of WSe₂ Monolayer

To explore how the adsorption of Cu, Ni, and Fe atoms affects the electronic properties of a WSe₂ monolayer, Density of States (DOS) and Projected Density of States (PDOS) calculations were conducted for the most stable adsorption configurations of these transition metal (TM) atoms. The resulting DOS and PDOS plots show notable changes in the electronic properties of the WSe₂ monolayer upon adsorption of these atoms. Fig.(16)a) and (16)d) display the DOS and PDOS for the WSe₂ monolayer with Cu adsorption. Fig.(16)a), DOS curve indicates the

presence of continuous electronic states near the Fermi level (E_F), signifying that the WSe_2 monolayer's band gap decreases from its pristine value of 1.27 eV to zero when Cu is adsorbed. This reduction means the WSe_2 monolayer transitions from semiconductors to metallic states. Fig.(16)d) and (16)g), PDOS reveal that the 3d orbitals of the Cu atom, the 5d orbitals of the W atom, and the 4p orbitals of the Se atom primarily contribute to the DOS around the Fermi level. The significant overlap among these orbitals suggests strong hybridization, indicating the formation of covalent bonds between the Cu atom and the WSe_2 monolayer, drastically altering its electronic properties. For the WSe_2 monolayer with Ni adsorption, as depicted in Fig.(16)b) and (16)e), the DOS curve in Fig.(16)b) shows that the band gap of the WSe_2 monolayer decreases from 1.27 eV to 0.88 eV upon Ni adsorption. This suggests a change in the WSe_2 monolayer from a semiconductor to a narrow band gap semiconductor. From Fig.(16)e) and (16)h), PDOS indicate that the 3d orbitals of the Ni atom, along with the 5d orbitals of the W atom and the 4p orbitals of the Se atom, contribute significantly to the DOS. The overlap of these orbitals indicates strong hybridization between the Ni atom and the WSe_2 monolayer, leading to covalent bond formation, which substantially changes the WSe_2 monolayer's electronic properties upon Ni adsorption. Fig.(16)c) and (16)f) illustrate the impact of Fe adsorption on the electronic properties of the WSe_2 monolayer. The DOS curve in Fig.(16)c) shows the band gap of the WSe_2 monolayer reducing to zero upon Fe adsorption, indicating a transition from a semiconductor to a metallic state, similar to the effect of Cu adsorption. From Fig.(16)f) and (16)i), PDOS reveal that the 3d orbitals of the Fe atom, the 5d orbitals of the W atom, and the 4p orbitals of the Se atom are the significant contributors to the DOS around the Fermi level. The overlap among these orbitals suggests strong hybridization between the Fe atom and the WSe_2 monolayer, resulting in covalent bond formation that significantly alters the electronic properties of the WSe_2 monolayer upon Fe adsorption. In summary, the adsorption of Cu, Ni, and Fe atoms onto the WSe_2 monolayer significantly affects its electronic properties. Cu and Fe adsorption reduces the band gap to zero, transitioning the monolayer from a semiconductor to a metallic state. Ni adsorption narrows the band gap from 1.27 eV to 0.88 eV, turning the WSe_2 monolayer into a narrow band gap semiconductor. The PDOS analysis shows that the 3d orbitals of the transition metal atoms, the 5d orbitals of W atoms, and the 4p orbitals of Se atoms primarily contribute to the DOS near the Fermi level. The significant overlap and strong hybridization among these orbitals indicate the formation of covalent bonds between the transition metal atoms and the WSe_2 monolayer, creating new electronic states within the electronic band structure and altering the monolayer's electronic properties.

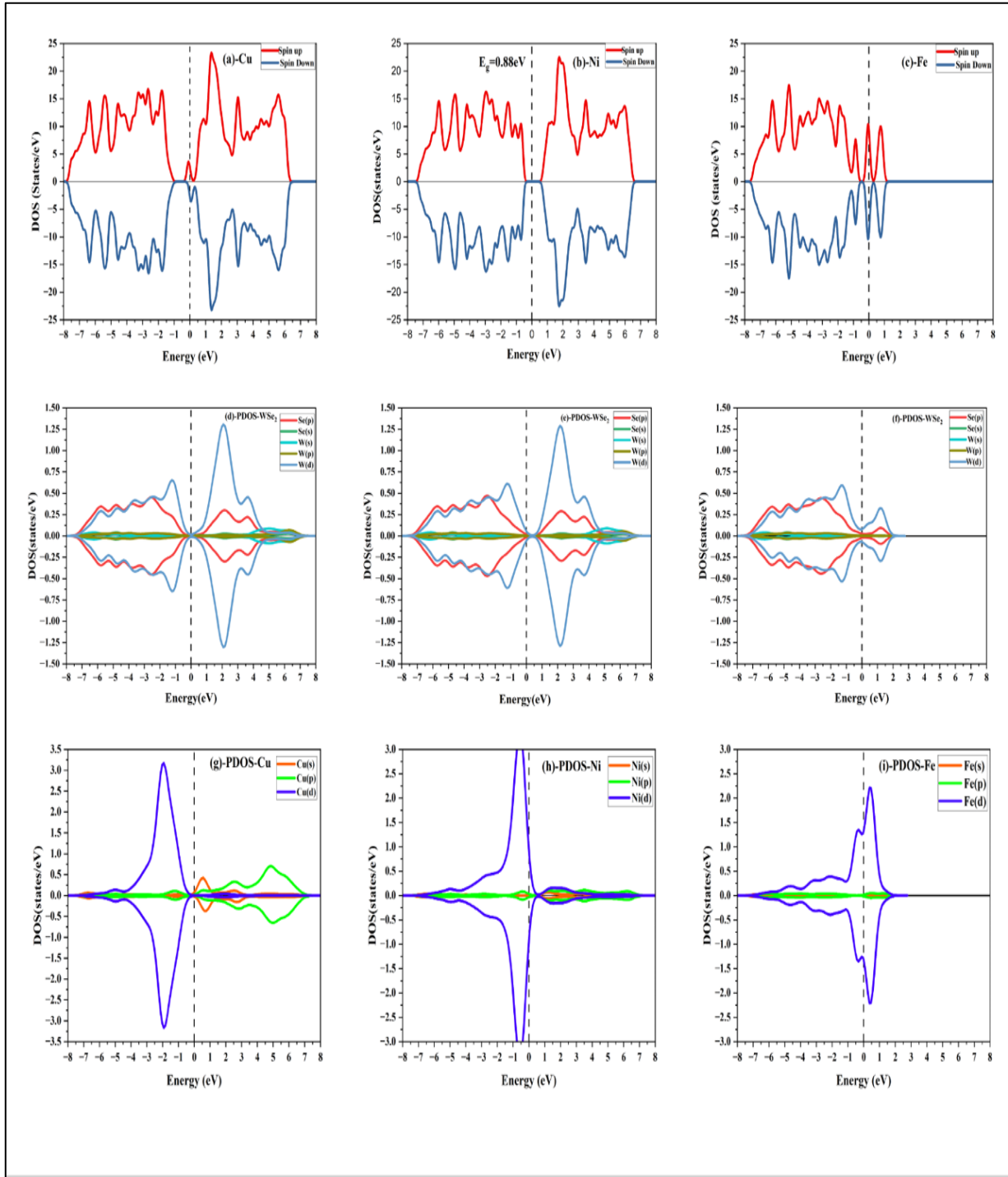


Fig. (16) a),b),c) illustrates plotted DOS curve, d),e),f) plotted WSe₂ PDOS and g),h), i) plotted Cu, Ni, Fe PDOS curve for the Cu, Ni and Fe decorated WSe₂ monolayer respectively.

The strong hybridization and covalent bond formation suggest that the adsorption process is energetically favourable despite the initially endothermic nature of Cu adsorption. The relatively high adsorption energies indicate robust interactions between the transition metal atoms and the WSe₂ monolayer, consistent with observed structural deformations and changes

in bond lengths upon adsorption. In conclusion, the adsorption of transition metal atoms (Cu, Ni, and Fe) onto the WSe₂ monolayer induces significant modifications in its electronic properties. The reduction or closure of the band gap and the emergence of new electronic states are mainly due to the strong hybridization and covalent bonding between the transition metal atoms and the WSe₂ monolayer. These findings demonstrate the potential for tuning the electronic properties of WSe₂ monolayers through the adsorption of different transition metal atoms, which could be helpful for various applications in electronics, optoelectronics, and catalysis.

3.2.5 Charge Density Difference Analysis

Charge density difference calculations were performed to analyse the charge transfer mechanism between transition metal (TM) atoms and a WSe₂ monolayer upon adsorption for the most stable adsorption configurations. This analysis provides qualitative insights into the nature and extent of charge transfer during adsorption. The charge density difference, calculated per equation(12), is illustrated in Fig.(17) for the most stable adsorption configurations. In these diagrams, red regions indicate areas of charge gain, while blue regions represent areas of charge loss. For the Cu-decorated WSe₂ monolayer, the charge density difference diagram (Fig.(17)a)) reveals distinct blue and red regions at the adsorption site. This suggests significant charge redistribution upon Cu adsorption. The Cu atom acts as an electron donor, transferring charge to the WSe₂ monolayer, which functions as an electron acceptor. This charge transfer results in charged species forming at the interface, creating an electrostatic attraction that enhances the interaction between the Cu atom and the WSe₂ monolayer. Similarly, in the case of Ni adsorption, the charge density difference diagram (Fig. (17)b)) displays blue and red regions at the adsorption site. The blue regions around the Ni atom indicate areas of charge loss, while the red regions on the WSe₂ monolayer signify areas of charge gain. This pattern confirms that the Ni atom donates electrons to the WSe₂ monolayer, reinforcing the electron donor-acceptor relationship. This charge transfer mechanism strengthens the bonding between the Ni atom and the WSe₂ monolayer, contributing to the stability of the adsorbed configuration. For the Fe-decorated WSe₂ monolayer, the charge density difference diagram (Fig. (17)c)) also shows blue and red regions at the adsorption site, consistent with the behaviour observed for Cu and Ni. The Fe atom loses electrons (indicated by the blue regions), while the WSe₂ monolayer gains electrons (indicated by the red regions). This charge transfer mechanism confirms that Fe atoms, like Cu and Ni atoms, act as electron

donors, transferring charge to the WSe₂ monolayer. In all case Cu, Ni, and Fe adsorption, the TM atoms act as electron donors, transferring charge to the WSe₂ monolayer, which acts as an electron acceptor. This charge transfer mechanism is crucial for understanding the changes in electronic properties observed upon TM adsorption. The charge transfer creates charged species at the adsorption site, resulting in an electrostatic attraction between the TM atoms and the WSe₂ monolayer. This interaction enhances the stability of the adsorbed configuration and contributes to the formation of covalent bonds. The presence of charged species also increases the mobility of charge carriers within the WSe₂ monolayer. This increased mobility leads to a higher electron current density, enhancing the conductivity of the WSe₂ monolayer. The increase in conductivity is directly related to the reduction in the band gap observed in the DOS analysis. The charge transfer from the TM atoms to the WSe₂ monolayer introduces new electronic states within the band structure, thereby reducing the band gap and altering the material's electronic properties. The analysis provides a detailed explanation for the bond formation and changes in electronic properties suggested by the adsorption and DOS studies. The strong hybridization between the TM atoms and the WSe₂ monolayer, facilitated by the charge transfer, leads to new electronic states. This hybridization and the resulting covalent bonding are responsible for the observed reduction in the band gap and the transition of the WSe₂ monolayer from a semiconductor to a metallic state (for Cu and Fe) or a narrow band gap semiconductor (for Ni). In conclusion, the analysis confirms that the TM atoms (Cu, Ni, and Fe) act as electron donors, transferring charge to the WSe₂ monolayer. This charge transfer mechanism stabilizes the adsorbed configurations and significantly alters the electronic properties of the WSe₂ monolayer by introducing new electronic states and reducing the band gap.

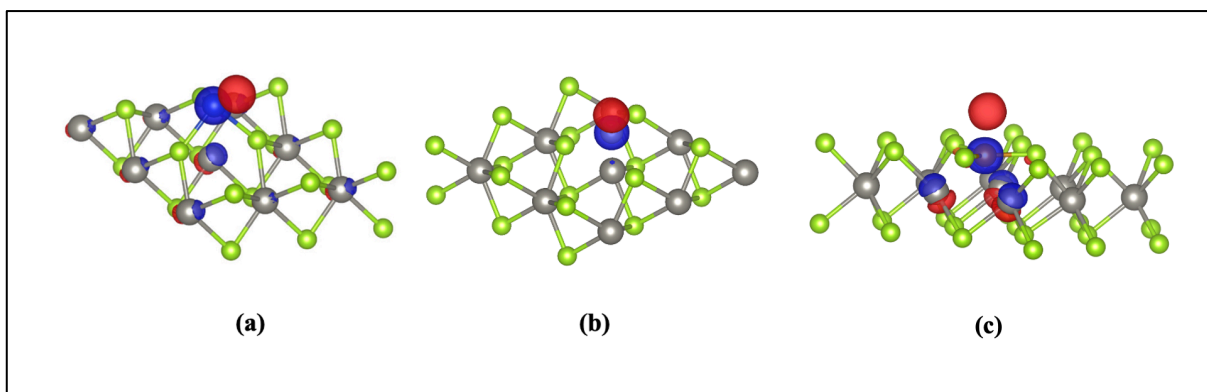


Fig.(17) Charge density diagram for a)Cu, b)Ni and c) Fe decorated onto the WSe₂ monolayer respectively.

CONCLUSION AND FUTURE SCOPE

Our investigation employed first principle calculations to examine the adsorption of transition metal (TM) atoms, specifically copper (Cu), nickel (Ni), and iron (Fe), onto a tungsten diselenide (WSe₂) monolayer. This study provided significant insights into the interactions between these TM atoms and the WSe₂ monolayer, particularly focusing on changes in electronic properties, charge transfer, and structural geometry following adsorption. We assessed three potential adsorption sites for each TM atom and determined the most favorable configurations for adsorption.

Our results revealed that Cu, Ni, and Fe atoms preferentially adsorb onto specific sites on the WSe₂ monolayer, where they form strong interactions that substantially influence the monolayer's electronic properties. Notably, the adsorption of Cu and Fe led to a significant reduction in the band gap, effectively transforming the WSe₂ monolayer into a metallic state. In contrast, the adsorption of Ni resulted in a narrower band gap semiconductor.

Charge transfer analysis indicated that the TM atoms donated electrons to the WSe₂ monolayer, contributing to the observed alterations in the electronic structure. This electron donation suggests the formation of an n-type material, enhancing the WSe₂ monolayer's potential for various electronic applications.

Furthermore, our study observed strong orbital overlap between the TM atoms and the WSe₂ monolayer, indicating the formation of covalent bonds. This covalent bonding ensures stable electronic properties and robust interactions between the TM atoms and the monolayer, further enhancing the material's potential for stable and efficient electronic applications.

The findings underscore the considerable potential of WSe₂ monolayers in electronic applications where precise control over material properties is crucial. By tailoring the band gap through the adsorption of TM atoms, it is possible to design devices with specific conductive properties, such as transistors and sensors. Additionally, the mechanisms of charge transfer and orbital hybridization observed in this study could facilitate the development of spintronic devices and flexible electronics. These findings open new avenues for applications in energy harvesting and optoelectronics.

Overall, our study highlights the promising potential of WSe₂ monolayers in various electronic applications that require narrow-band semiconductors and zero-band gap materials. The ability

to control electronic properties through TM atom adsorption makes WSe₂ monolayers a versatile material for a wide range of technological applications. This capability enables the design of devices with tailored electronic properties, including transistors, sensors, and spintronic devices, as well as applications in energy harvesting and flexible electronics. By leveraging the unique interactions between TM atoms and the WSe₂ monolayer, our study provides a pathway for developing advanced materials with highly controlled electronic characteristics, suitable for next-generation electronic devices.

REFERENCES

- [1] K. T. Ramesh and K. Ramesh, *Nanomaterials*: Springer, 2009.
- [2] B. Singh, H. Zeng, C. Guo, and W. Cai, *Nanomaterials*: Springer, 2013.
- [3] D. Vollath, *Nanomaterials: an introduction to synthesis, properties and applications*: John Wiley & Sons, 2013.
- [4] A. B. Asha and R. Narain, "Nanomaterials properties," in *Polymer science and nanotechnology*, ed: Elsevier, 2020, pp. 343-359.
- [5] J. T. Lue, "Physical properties of nanomaterials," *Encyclopedia of nanoscience and nanotechnology*, vol. 10, pp. 1-46, 2007.
- [6] N. Baig, I. Kammakakam, and W. Falath, "Nanomaterials: A review of synthesis methods, properties, recent progress, and challenges," *Materials Advances*, vol. 2, pp. 1821-1871, 2021.
- [7] W. A. D. M. Jayathilaka, K. Qi, Y. Qin, A. Chinnappan, W. Serrano-García, C. Baskar, *et al.*, "Significance of nanomaterials in wearables: a review on wearable actuators and sensors," *Advanced Materials*, vol. 31, p. 1805921, 2019.
- [8] S. Yao, P. Swetha, and Y. Zhu, "Nanomaterial-enabled wearable sensors for healthcare," *Advanced healthcare materials*, vol. 7, p. 1700889, 2018.
- [9] R. Das, W. Zeng, C. Asci, R. Del-Rio-Ruiz, and S. Sonkusale, "Recent progress in electrospun nanomaterials for wearables," *APL bioengineering*, vol. 6, 2022.
- [10] S. Das, B. Sen, and N. Debnath, "Recent trends in nanomaterials applications in environmental monitoring and remediation," *Environmental Science and Pollution Research*, vol. 22, pp. 18333-18344, 2015.
- [11] K. Gajanan and S. Tijare, "Applications of nanomaterials," *Materials Today: Proceedings*, vol. 5, pp. 1093-1096, 2018.
- [12] S. A. Mazari, E. Ali, R. Abro, F. S. A. Khan, I. Ahmed, M. Ahmed, *et al.*, "Nanomaterials: Applications, waste-handling, environmental toxicities, and future challenges—A review," *Journal of Environmental Chemical Engineering*, vol. 9, p. 105028, 2021.
- [13] G. Ramalingam, P. Kathirgamanathan, G. Ravi, T. Elangovan, N. Manivannan, and K. Kasinathan, "Quantum confinement effect of 2D nanomaterials," in *Quantum Dots-Fundamental and Applications*, ed: IntechOpen, 2020.

- [14] G. Chen, J. Seo, C. Yang, and P. N. Prasad, "Nanochemistry and nanomaterials for photovoltaics," *Chemical Society Reviews*, vol. 42, pp. 8304-8338, 2013.
- [15] T. Edvinsson, "Optical quantum confinement and photocatalytic properties in two-, one- and zero-dimensional nanostructures," *Royal society open science*, vol. 5, p. 180387, 2018.
- [16] T. Yang, Y. Liu, H. Wang, Y. Duo, B. Zhang, Y. Ge, *et al.*, "Recent advances in 0D nanostructure-functionalized low-dimensional nanomaterials for chemiresistive gas sensors," *Journal of Materials Chemistry C*, vol. 8, pp. 7272-7299, 2020.
- [17] Z. Wang, T. Hu, R. Liang, and M. Wei, "Application of zero-dimensional nanomaterials in biosensing," *Frontiers in chemistry*, vol. 8, p. 320, 2020.
- [18] C. Daulbayev, F. Sultanov, B. Bakbolat, and O. Daulbayev, "0D, 1D and 2D nanomaterials for visible photoelectrochemical water splitting. A Review," *International Journal of Hydrogen Energy*, vol. 45, pp. 33325-33342, 2020.
- [19] E. Garnett, L. Mai, and P. Yang, "Introduction: 1D nanomaterials/nanowires," *Chemical reviews*, vol. 119, pp. 8955-8957, 2019.
- [20] T. Jin, Q. Han, Y. Wang, and L. Jiao, "1D nanomaterials: design, synthesis, and applications in sodium-ion batteries," *Small*, vol. 14, p. 1703086, 2018.
- [21] H. Zhang, M. Chhowalla, and Z. Liu, "2D nanomaterials: graphene and transition metal dichalcogenides," *Chemical Society Reviews*, vol. 47, pp. 3015-3017, 2018.
- [22] H. Jin, C. Guo, X. Liu, J. Liu, A. Vasileff, Y. Jiao, *et al.*, "Emerging two-dimensional nanomaterials for electrocatalysis," *Chemical reviews*, vol. 118, pp. 6337-6408, 2018.
- [23] H. Zhang, H.-M. Cheng, and P. Ye, "2D nanomaterials: beyond graphene and transition metal dichalcogenides," *Chemical Society Reviews*, vol. 47, pp. 6009-6012, 2018.
- [24] H. Gleiter, "Nanocrystalline materials," in *Advanced Structural and Functional Materials: Proceedings of an International Seminar Organized by Deutsche Forschungsanstalt für Luft-und Raumfahrt (DLR), Köln, June 1991*, 1991, pp. 1-37.
- [25] P. M. Ajayan, L. S. Schadler, and P. V. Braun, *Nanocomposite science and technology*: John Wiley & Sons, 2006.
- [26] X. Pan, L. Bai, H. Wang, Q. Wu, H. Wang, S. Liu, *et al.*, "Metal-organic-framework-derived carbon nanostructure augmented sonodynamic cancer therapy," *Advanced materials*, vol. 30, p. 1800180, 2018.
- [27] C. Verma, E. Berdimurodov, D. K. Verma, K. Berdimuradov, A. Alfantazi, and C. Hussain, "3D nanomaterials: The future of industrial, biological, and environmental applications," *Inorganic Chemistry Communications*, p. 111163, 2023.

- [28] C. Zhu, T. Liu, F. Qian, W. Chen, S. Chandrasekaran, B. Yao, *et al.*, "3D printed functional nanomaterials for electrochemical energy storage," *Nano Today*, vol. 15, pp. 107-120, 2017.
- [29] D. Van Gough, A. T. Juhl, and P. V. Braun, "Programming structure into 3D nanomaterials," *Materials today*, vol. 12, pp. 28-35, 2009.
- [30] A. Murali, G. Lokhande, K. A. Deo, A. Brokesh, and A. K. Gaharwar, "Emerging 2D nanomaterials for biomedical applications," *Materials Today*, vol. 50, pp. 276-302, 2021.
- [31] C. Tan, X. Cao, X.-J. Wu, Q. He, J. Yang, X. Zhang, *et al.*, "Recent advances in ultrathin two-dimensional nanomaterials," *Chemical reviews*, vol. 117, pp. 6225-6331, 2017.
- [32] V. S. Bhati, M. Kumar, and R. Banerjee, "Gas sensing performance of 2D nanomaterials/metal oxide nanocomposites: A review," *Journal of Materials Chemistry C*, vol. 9, pp. 8776-8808, 2021.
- [33] C. Wang, K. Xia, H. Wang, X. Liang, Z. Yin, and Y. Zhang, "Advanced carbon for flexible and wearable electronics," *Advanced materials*, vol. 31, p. 1801072, 2019.
- [34] A. Ahmed, S. Sharma, B. Adak, M. M. Hossain, A. M. LaChance, S. Mukhopadhyay, *et al.*, "Two-dimensional MXenes: New frontier of wearable and flexible electronics," *InfoMat*, vol. 4, p. e12295, 2022.
- [35] H. Qiao, H. Liu, Z. Huang, R. Hu, Q. Ma, J. Zhong, *et al.*, "Tunable electronic and optical properties of 2D monoelemental materials beyond graphene for promising applications," *Energy & Environmental Materials*, vol. 4, pp. 522-543, 2021.
- [36] A. K. Geim, "Graphene: status and prospects," *science*, vol. 324, pp. 1530-1534, 2009.
- [37] H. Huang, X. Fan, D. J. Singh, and W. Zheng, "Recent progress of TMD nanomaterials: phase transitions and applications," *Nanoscale*, vol. 12, pp. 1247-1268, 2020.
- [38] J. An, X. Zhao, Y. Zhang, M. Liu, J. Yuan, X. Sun, *et al.*, "Perspectives of 2D materials for optoelectronic integration," *Advanced Functional Materials*, vol. 32, p. 2110119, 2022.
- [39] J. Zha, M. Luo, M. Ye, T. Ahmed, X. Yu, D. H. Lien, *et al.*, "Infrared photodetectors based on 2D materials and nanophotonics," *Advanced Functional Materials*, vol. 32, p. 2111970, 2022.
- [40] Z. Cheng, R. Cao, K. Wei, Y. Yao, X. Liu, J. Kang, *et al.*, "2D materials enabled next-generation integrated optoelectronics: from fabrication to applications," *Advanced Science*, vol. 8, p. 2003834, 2021.

- [41] X. Hu, L. Yan, L. Ding, N. Zheng, D. Li, T. Ji, *et al.*, "Structural regulation and application of transition metal dichalcogenide monolayers: Progress and challenges," *Coordination Chemistry Reviews*, vol. 499, p. 215504, 2024.
- [42] W. Alfalasi, Y. P. Feng, and N. Tit, "Designing a functionalized 2D-TMD (MoX₂, X= S, Se) hosting half-metallicity for selective gas-sensing applications: Atomic-scale study," *Acta Materialia*, vol. 246, p. 118655, 2023.
- [43] K. B. M. Ismail, M. Arun Kumar, S. Mahalingam, J. Kim, and R. Atchudan, "Recent advances in molybdenum disulfide and its nanocomposites for energy applications: Challenges and development," *Materials*, vol. 16, p. 4471, 2023.
- [44] Z. Cui, K. Yang, Y. Shen, Z. Yuan, Y. Dong, P. Yuan, *et al.*, "Toxic gas molecules adsorbed on intrinsic and defective WS₂: gas sensing and detection," *Applied Surface Science*, vol. 613, p. 155978, 2023.
- [45] B. A. Foutty, C. R. Kometter, T. Devakul, A. P. Reddy, K. Watanabe, T. Taniguchi, *et al.*, "Mapping twist-tuned multiband topology in bilayer WSe₂," *Science*, vol. 384, pp. 343-347, 2024.
- [46] T. Ahmed, J. Zha, K. K. Lin, H. C. Kuo, C. Tan, and D. H. Lien, "Bright and Efficient Light-Emitting Devices Based on 2D Transition Metal Dichalcogenides," *Advanced Materials*, vol. 35, p. 2208054, 2023.
- [47] W. Ahmad, A. K. Tareen, K. Khan, M. Khan, Q. Khan, Z. Wang, *et al.*, "A review of the synthesis, fabrication, and recent advances in mixed dimensional heterostructures for optoelectronic devices applications," *Applied Materials Today*, vol. 30, p. 101717, 2023.
- [48] S. Aftab and H. H. Hegazy, "Emerging Trends in 2D TMDs Photodetectors and Piezo-Phototronic Devices," *Small*, vol. 19, p. 2205778, 2023.
- [49] A. Hayat, M. Sohail, A. El Jery, K. M. Al-Zaydi, S. Raza, H. Ali, *et al.*, "Recent advances, properties, fabrication and opportunities in two-dimensional materials for their potential sustainable applications," *Energy Storage Materials*, vol. 59, p. 102780, 2023.
- [50] A. Azam, J. Yang, W. Li, J.-K. Huang, and S. Li, "Tungsten diselenides (WSe₂) quantum dots: Fundamental, properties, synthesis and applications," *Progress in Materials Science*, vol. 132, p. 101042, 2023.


- [51] Chen GX, Li HF, Yang X, Wen JQ, Pang Q, Zhang JM. Adsorption of 3d transition metal atoms on graphene-like gallium nitride monolayer: A first-principles study. *Superlattices Microstruct* 2018; 115: 108–115.
- [52] Ju W, Li T, Zhou Q, Li H, Li X, Ma D. Adsorption of 3d transition-metal atom on InSe monolayer: A first-principles study. *Comput Mater Sci* 2018; 150: 33–41.
- [53] Ju W, Li T, Zhou Q, Li H, Li X, Ma D. Adsorption of 3d transition-metal atom on InSe monolayer: A first-principles study. *Comput Mater Sci* 2018; 150: 33–41.
- [54] Wang Y, Wang B, Huang R, Gao B, Kong F, Zhang Q. First-principles study of transition-metal atoms adsorption on MoS₂ monolayer. *Physica E Low Dimens Syst Nanostruct* 2014; 63: 276–282.
- [55] Zhao B, Li CY, Liu LL *et al.* Adsorption of gas molecules on Cu impurities embedded monolayer MoS₂: A first-principles study. *Appl Surf Sci* 2016; 382: 280–287.
- [56] Bagayoko D. Understanding density functional theory (DFT) and completing it in practice. *AIP Adv* 2014; 4.
- [57] te Vrugt M, Löwen H, Wittkowski R. Classical dynamical density functional theory: from fundamentals to applications. *Advances in Physics* 69 2020 121–247.
- [58] Obot IB, Macdonald DD, Gasem ZM. Density functional theory (DFT) as a powerful tool for designing new organic corrosion inhibitors: Part 1: An overview. *Corrosion Science* 99 2015 1–30.
- [59] Verma P, Truhlar DG. Status and Challenges of Density Functional Theory. *Trends in Chemistry* 2 2020 302–318.
- [60] Kohn W, Becke AD, Parr RG. *Density Functional Theory of Electronic Structure*. 1996.
- [61] Carnimeo I, Affinito F, Baroni S *et al.* Quantum ESPRESSO: One Further Step toward the Exascale. *J Chem Theory Comput* 2023; 19: 6992–7006.
- [62] Matsugatani A, Ono S, Nomura Y, Watanabe H. qeirreps: An open-source program for Quantum ESPRESSO to compute irreducible representations of Bloch wavefunctions ☆,☆☆. *Comput Phys Commun* 2021; 264: 107948.
- [63] Malet F, Mirschink A, Giesbertz KJH, Wagner LO, Gori-Giorgi P. Exchange-correlation functionals from the strong interaction limit of DFT: Applications to model


- chemical systems. *Physical Chemistry Chemical Physics*, Royal Society of Chemistry 2014, 14551–14558.
- [64] Domagała M, Jabłoński M, Dubis AT, Zabel M, Pfitzner A, Palusiak M. Testing of Exchange-Correlation Functionals of DFT for a Reliable Description of the Electron Density Distribution in Organic Molecules. *Int J Mol Sci* 2022; 23.
- [65] Tromer RM, Ribeiro LA, Galvão DS. A DFT study of the electronic, optical, and mechanical properties of a recently synthesized monolayer fullerene network. *Chem Phys Lett* 2022; 804.
- [66] Gundelach L, Fox T, Tautermann CS, Skylaris CK. Protein-ligand free energies of binding from full-protein DFT calculations: convergence and choice of exchange-correlation functional. *Physical Chemistry Chemical Physics* 2021; 23: 9381–9393.
- [67] Deepthi Jayan K, Sebastian V. Ab initio DFT determination of structural, mechanical, optoelectronic, thermoelectric and thermodynamic properties of RbGeI₃ inorganic perovskite for different exchange-correlation functionals. *Mater Today Commun* 2021; 28.
- [68] Garrity KF, Bennett JW, Rabe KM, Vanderbilt D. Pseudopotentials for high-throughput DFT calculations. *Comput Mater Sci* 2014; 81: 446–452.
- [69] Lai KK, Mishra SK, Panda G, Chakraborty SK, Samei ME, Ram B. A limited memory q-BFGS algorithm for unconstrained optimization problems. *J Appl Math Comput* 2021; 66: 183–202.
- [70] Andrei N. An adaptive scaled BFGS method for unconstrained optimization. *Numer Algorithms* 2018; 77: 413–432.

List of Publications and Proof



Scopus Index

Search [Authors & Editors](#) [Account](#)



Book series

Springer Proceedings in Physics

About this book series


Indexed by Scopus

The series Springer Proceedings in Physics, founded in 1984, is devoted to timely reports of state-of-the-art developments in physics and related sciences. Typically based on material presented at conferences, workshops and similar scientific meetings, volumes published in this series will constitute a comprehensive up to date source of reference on a field or subfield of relevance in contemporary physics. Proposals must include the following: — [show all](#)

Publish with us

- [Submission guidelines](#)
- [Open access publishing](#)
- [Policies and ethics](#)

Contact the Publishing Editor

[Zachary Evenson](#) 

[Download book proposal form](#)


Electronic ISSN Print ISSN

1867-4941 0930-8989

Book titles in this series


[Proceedings of the 9th International Symposium on Hydrogen Energy, Renewable Energy and Materials](#)

HEREM23, Oct. 13-14, 2023, Bangkok, Thailand



International Conference on Atomic, Molecular, Material, Nano and Optical Physics with Applications (ICAMNOP-2023)

Organized by: Department of Applied Physics, Delhi Technological University Delhi-110042, India
December 20th-22nd, 2023



- HOME
- CONFERENCE
- COMMITTEE
- SPEAKERS
- PUBLICATION
- REGISTRATION
- ABSTRACTS
- ACCOMMODATION
- TOUR
- GALLERY
- CONTACT US

[Login](#)

About The Conference

International Conference on Atomic, Molecular, Material, Nano and Optical Physics with Applications (ICAMNOP-2023) will focus on developments in atomic, molecular, material, Nano and Optical Physics which have proved to be powerful science supporting many other areas of science & technology, including industrial, information, energy, global Change, defense, health and medical environmental, space and transportation technology.

[Read More >>](#)

PLAGARISM REPORT

PAPER NAME

Thesis-2 edited .docx

WORD COUNT

10008 Words

CHARACTER COUNT

61022 Characters

PAGE COUNT

41 Pages

FILE SIZE

10.2MB

SUBMISSION DATE

Jun 2, 2024 12:59 PM GMT+5:30

REPORT DATE

Jun 2, 2024 12:59 PM GMT+5:30

● 9% Overall Similarity

The combined total of all matches, including overlapping sources, for each database.

- 5% Internet database
- 4% Publications database
- Crossref database
- Crossref Posted Content database
- 6% Submitted Works database

● Excluded from Similarity Report

- Bibliographic material
- Quoted material
- Cited material
- Small Matches (Less than 10 words)